

ABSTRACT

Title of Thesis: USE OF MILLIGRAM-SCALE FLAME
CALORIMETRY FOR CHARACTERIZING
FLAMMABILITY OF FABRIC SAMPLES
WITH FLAME RETARDANT TREATMENTS

Thomas William Roche, Master of Science, 2023

Thesis Directed By: Assistant Professor Fernando Raffan-Montoya,
Fire Protection Engineering

The fire hazard associated with fabrics threatens everyone's safety, and the current standards used to reduce those hazards are expensive and time-consuming. Fabrics are a key component in clothing, upholstery, and carpentry and are present in nearly every built environment. The inherent flammability of fabrics leads to the application of flame-retardant treatments on nearly all commercial fabric products. Recently, environmental, economic and performance concerns have driven research to develop new flame retardants across a variety of materials. The military industry in particular has focused recent research efforts on flame retardant treatments for fabrics, given the challenging environments that military uniforms must endure. Current methods for testing performance of novel flame retardants, such as the Cone Calorimeter and Microscale Combustion Calorimeter can be prohibitively expensive or only provide a limited understanding of flame-retardant action. Fabrics present additional testing challenges due to their low density and thickness, effectively reducing the amount of fuel available for testing. A novel apparatus, the Milligram-scale Flame Calorimeter (MFC), has been used to test flame retardants in polymeric

materials, successfully capturing gas-phase activity and with favorable comparison to Cone Calorimeter results. This study aims to expand the use of the MFC to the testing of fabrics and flame-retardant treated fabrics. Optimization tests were run to find the optimal number of fabric layers and best method for preparing samples for use in MFC. Subsequently, cotton fabrics (untreated and treated with phosphoric acid), as well as Nylon fabrics (untreated and treated with tannic acid) were characterized with MFC, and results were compared to those from the Microscale Combustion Calorimeter and Cone Calorimeter. The MFC showed similar trends in the onset of ignition, peak heat release rate, average heat release rate, char yield, and heat of combustion for the untreated fabrics with the Cone Calorimeter and Microscale Combustion Calorimeter results. The results for the flame-retarded fabrics are inconclusive and require additional testing, though the observations of the condensed-phase and gas-phase activity for the MFC samples does provide important insights on how the mechanism for the flame retardants operate.

USE OF MILLIGRAM-SCALE FLAME CALORIMETRY FOR
CHARACTERIZING FLAMMABILITY OF FABRIC SAMPLES WITH
FLAME RETARDANT TREATMENTS

by

Thomas William Roche

Thesis submitted to the Faculty of the Graduate School of the
University of Maryland, College Park, in partial fulfillment
of the requirements for the degree of
Master of Science
2023

Advisory Committee:

Assistant Professor Fernando Raffan-Montoya, Chair

Professor Stanislav Stoiliarov

Dr. Alexander Morgan

© Copyright by
Thomas William Roche
2023

Acknowledgements

I would like to thank my family for their love and support not only through this past year but through all our years together. For every dark or frustrating moment I encounter, they each help to relieve my stress in their own wonderful ways. For John, as a brotherly role model and shoulder to lean on; for Michelle, with her positive reinforcement and realistic attitude; for my father and mother, who are endlessly self-sacrificing and willing to help at a moment's notice. I love you all.

I would like to thank my advisor, Dr. Fernando Raffan-Montoya, for his insight, patience and encouragement over this past year. His ability to communicate and pass on his understanding of fire phenomena, mechanical engineering, the graduate student experience, and life lessons are even more appreciated as his graduate student than an undergrad learning fluid dynamics. I was ecstatic when you were able to begin to road to professorship and will do everything I can to help you along that path. I'm proud to be your student and looking forward to earning my doctorate under your guidance.

I would like to thank Dr. Stanislav Stoiliarov for his assistance and wisdom on both the MFC and the logistics of graduate studies. His experience in what is expected of both student and professor has helped both Fernando and I excel in our new roles, and his insight on how to progress our research on the MFC has been pivotal. We couldn't have done it without you.

I would like to thank Joe Pudvah for his assistance in conducting tests during the last part of thesis writing. Joe's ability to learn quickly, ask inquisitive questions, and methodically follow instructions made him even better at running the last few

experiments than I was. I look forward to seeing you join the department as an undergraduate student next year.

I would like to thank Jacques A. De Beer for helping me in the early stages of the MFC research and graduate studies. He's been a shining example of the work ethic and logical expertise required of researchers through both my undergraduate and now graduate career. I wish him the best in his future endeavors as he graduates.

I want to thank my friends and colleagues in the FPE graduate department for their fellowship and camaraderie through both classes and research. Sofia, Kelliann, Genevieve, Alexis, Jeff, Zishan, Dave, Saleel, Alec, Yiren, Farnaz, Bekah, and Sangkyu, you all brightened up the office. Thank you all for the past year together.

Finally, I would like to thank Dr. Alex Morgan, Sourabh Kulkarni, and Dr. Ramaswamy Nagarajan for their assistance in providing samples and data for the thesis. Thank you all for your time and expertise on the fabrics and the burn behaviors observed. Additional thanks to Dr. Alex Morgan for providing his time to serve on my thesis committee. I am grateful to you all and look forward to working with you on the HEROES project.

Table of Contents

Acknowledgements	ii
Table of Contents	iv
List of Tables	vi
List of Figures	vii
List of Abbreviations	xi
1 Introduction and Background Information	1
1.1 Overview	1
1.2 Bench Scale Flammability Test Methods for Fabrics	3
1.2.1 Oxygen Consumption Calorimetry	3
1.2.2 Cone Calorimeter	4
1.2.3 Microscale Combustion Calorimeter	6
1.2.4 Milligram-Scale Flame Calorimeter	8
1.3 Flame Behavior and Flame-Retardant Fabric Treatment Background	13
1.4 Objectives	16
2 Updates to Milligram-scale Flame Calorimeter Design	18
2.1 Igniter Power Supply	18
2.2 Temperature Repeatability	21
2.3 New Coupler for Glass/Cone Connection	23
2.4 Comparison to Previous MFC data	25
3 Experimental Design	29
3.1 Fabric Origins and Flame-Retardant Application	29
3.2 Cone Calorimetry Methodology	32
3.2.1 Cone Calorimeter Setup	32
3.2.2 Cone Calorimeter Post-Processing	33
3.3 MCC Methodology	34
3.3.1 MCC Setup	34
3.3.2 MCC Post-Processing	34
3.4 MFC Setup	34
3.4.1 MFC Layer Depth	35
3.4.2 MFC Sample Packing	38
3.4.3 MFC Setup Information	41
3.4.4 MFC Post-Processing	43
4 Results	44
4.1 Cone Calorimeter Results	44
4.2 MCC Results	49
4.3 MFC Results	54
5 Comparative Analysis and Discussion	60
5.1 Onset of Ignition	60
5.2 Char Yield	67
5.3 Peak and Average HRR	68
5.4 Heat of Combustion	73
6 Conclusion and Future Work	78
6.1 Conclusion	78

6.2	Future Work	79
7	Bibliography	81

List of Tables

Table 2.1: Cotton Tests using the Original Pyrolyzer (the pyrolyzer used for the other tests in the current study) and the New Pyrolyzer	23
Table 2.2: Current MFC results vs. De Beer's MFC Results for PMMA and PVC [28]	27
Table 3.1: Fabric and Flame Retardant Chemical Line Structures and Other Info	31
Table 3.2: Maximum Change in Oxygen Concentration for Multiple Layers of Cotton	37
Table 4.1: Summary of Cone Calorimeter Results	49
Table 4.2: Summary of MCC Results.....	54
Table 4.3: Summary of MFC Results	57

List of Figures

Figure 1.1: Cone Calorimeter Design Summary [21].....	5
Figure 1.2: Schematic Drawing of Microscale Combustion Calorimeter (MCC) [31] 7	
Figure 1.3: Schematic Diagram of the MFC and its Major Systems [17]	9
Figure 2.1: Igniter Power Captured by Temperature Increase in Pyrolyzer	19
Figure 2.2: Pyrolyzer Temperature with and without Igniter on during first 60 Seconds	20
Figure 2.3: Pyrolyzer Temperature between two Pyrolyzers.....	22
Figure 2.4: Schematic Cross Section of the Seal (Left), Top-Down View of the Seal (Right).....	24
Figure 2.5: Diagram of the Inflatable Seal System.....	25
Figure 2.6: Average HRR curves for PMMA (disk) and PVC (disk) for current MFC (left) and De Beer’s Results (right) [17].....	26
Figure 3.1: Chemical Structure of the Cotton with Phosphoric Flame Retardant and Nylon with Tannic Flame Retardant.....	32
Figure 3.2: Oxygen Concentration for Burning 1 Layer, 2 Layers, and 4 Layers of Cotton.....	36
Figure 3.3: Flame Height and Behavior for 1 Layer (a), 2 Layers (b), and 4 Layers of Cotton (c)	38
Figure 3.4: 4 Layers of Cotton packed into the crucible with the Ring Method (Left) and the Tamper Method (Right)	39
Figure 3.5: HRR for 4 Layers of Cotton with the Tamper Method and the Ring Method	40

Figure 3.6: Error in HRR for 4 Layers of Cotton with the Tamper Method and the Ring Method	41
Figure 3.7: MFC Fabric Samples, (from left to right) Cotton Control, PA Cotton, Nylon Control, TA Nylon.....	42
Figure 3.8: Pyrolyzer temperature during the typical MFC experiment.....	Error!
Bookmark not defined.	
Figure 4.1: Cone Calorimeter Charred Remains for Control Cotton (a), PA Cotton (b), Control Nylon (c), and TA Nylon (d) samples [48].....	45
Figure 4.2: Cone Calorimeter HRR curves for Control Cotton (a), PA Cotton (b) Control Nylon (c), and TA Nylon (d) [48]	46
Figure 4.3: Average HRR for all materials in the Cone Calorimeter	47
Figure 4.4: MCC HRR Curves for Control Cotton (a), PA Cotton (b), Control Nylon (c), and TA Nylon (d) [49].....	50
Figure 4.5: Average HRR for all materials in the MCC.....	52
Figure 4.6: MCC Charred remains for Cotton Control (a), PA Cotton (b), Nylon Control (c), and TA Nylon (d) [49]	53
Figure 4.7: MFC HRR Curves for Cotton Control (a), PA Cotton (b), Nylon Control (c), and TA Nylon (d)	55
Figure 4.8: Average HRR for all materials in the MFC	57
Figure 4.9: MFC Charred remains for Cotton Control (a), Nylon Control (b),PA Cotton (c), and TA Nylon (d)	59
Figure 5.1: Onset of Ignition for Cone (right axis), MFC, and MCC (left axis) Tests across all Fabrics (assuming thermally thin Cone Tests).....	62

Figure 5.2: Onset of Ignition for Cone (right axis), MFC, and MCC (left axis) Tests across all Fabrics (assuming thermally thick Cone Tests).....	63
Figure 5.3: Relative Change in Onset of Ignition between the Control to the Flame-Retarded Fabrics, Calculated using Equation (8) (Assuming Thermally Thin Cone Samples).....	64
Figure 5.4: Relative Change in Onset of Ignition from the Control to the Flame-Retarded Fabrics, Calculated using Equation (8) (Assuming Thermally Thick Cone Samples).....	65
Figure 5.5: Char Yield for Cone, MFC, and MCC Tests across all Fabrics.....	68
Figure 5.6: Peak HRR for Cone, MFC, and MCC tests for all fabrics normalized by area.....	70
Figure 5.7: Relative Change in pHRR from the Control fabrics to the Flame-Retarded Fabrics, Calculated using Equation (8).....	71
Figure 5.8: Average HRR for Cone, MFC, and MCC tests for all fabrics normalized by area.....	72
Figure 5.9: Relative Change in aHRR from the Control fabrics to the Flame-Retarded Fabrics, Calculated using Equation (8).....	73
Figure 5.10: HOC per initial mass for Cone, MFC, and MCC tests for all fabrics	74
Figure 5.11: HOC per gasified mass for Cone, MFC, and MCC tests for all fabrics.	74
Figure 5.12: Relative Change in HOC per initial mass from the Control fabrics to the Flame-Retarded Fabrics, Calculated using Equation (8)	76
Figure 5.13: Relative Change in HOC per gasified mass from the Control fabrics to the Flame-Retarded Fabrics, Calculated using Equation (8)	77

List of Abbreviations

MFC – Milligram-scale Flame Calorimeter

MCC – Microscale Combustion Calorimeter

THR – Total Heat Release

HOC – Heat of Combustion

DOD – Department of Defense

HRR – Heat Release Rate

pHRR – Peak Heat Release Rate

aHRR – Average Heat Release Rate

MLR – Mass Loss Rate

aMLR – Average Mass Loss Rate

T_{ign} – Ignition Temperature

T_{ext} – Extinction Temperature

t_{ign} – Ignition Time

t_{ext} – Extinction Time

Q''_{crit} – Critical heat flux for ignition

FAA – Federal Aviation Administration

NDIR – Nondispersive Infrared

OD – Outer Diameter

PA – Phosphoric Acid

TA – Tannic Acid

OMF – On mass of fabric

1 Introduction and Background Information

1.1 *Overview*

Fabrics are a key component of everyday life, including clothing, furniture, carpentry, etc. On the microscopic scale, fabrics are composed of long, thin filaments called fibers. Fibers can be naturally occurring (cotton, jute, flax, hemp, wool, silk, etc.) or synthetically produced polymers (nylon, polyester, acrylic, poly olefin, etc.). Several fibers spun together, either homogenous or heterogeneous blends, form yarn. Yarn is then woven into fabrics. Nearly all polymer and natural fibers are flammable. Fabrics therefore require the treatment of flame retardants to minimize the likelihood and severity of fire damage to people and property. In particular, military uniforms are expected to encounter environments including explosions and fire. The optimal uniform should reduce burn damage inflicted on the wearer from fire hazards rather than exacerbate those issues. However, military uniforms (and other fabrics) are also expected to be lightweight, environmentally friendly, economical, resilient to washing cycles, and meet several other criteria. Research into flame-retardant fabric treatments is ongoing to meet these criteria.

Flame-retardant fabric treatment research focuses on two major categories: creation of novel, fabric-compatible flame retardants and treatment methods, and testing flame-retardant treated fabrics in standardized experimental methods. While the methods for creating and applying new flame retardants have greatly expanded over the past several years [1-5], most of the methods for testing fabrics with flame retardant treatments have remained the same. Two of the standardized testing methods for

regulation and certification of fabrics for use in military applications include ASTM D6413, the Vertical Flame Test [6], and ASTM F1930, the Mannequin Flame Test [7].

The Vertical Flame Test provides qualitative information on the charring, dripping, and flame growth of a fabric sample exposed to an open flame. A Bunsen burner flame is placed beneath a vertical strip of fabric for 12 seconds, then removed. The flame time after removal is recorded, along with afterglow, dripping, the char length and char strength. This test is considered a pass/fail test, with limited quantitative insight. To pass the test, fabrics are required to extinguish before a certain period of time, not produce dripping, limit char growth or maintain a level of char strength, depending on the local standard. The qualitative nature of ASTM D6413 makes it difficult to predict how different fabrics and flame-retardant fabric treatments will perform.

The Mannequin Flame Test provides quantitative data on the human skin burn injury endured by an adult when wearing a single-layer clothing ensemble and exposed to direct flame impingement. Several heat sensors are placed on a full-body, fire-proof mannequin, along with a full-body garment. Eight burners are placed around the mannequin, providing an average exposure heat flux of 84 kW/m^2 for up to 20 seconds. The energy sensor data is converted into time-dependent heat flux values on the surface of the mannequin. The surface heat flux is computed into a one-dimensional temperature distribution within the “skin” of the mannequin using a numerical solution of the Fourier Field equation. This temperature distribution is used to calculate the burn injuries sustained at different parts of the body. The Mannequin Test provides important information on the expected protection an outfit will provide during a fire

hazard with the adjustable exposure time allowing for multiple potential scenarios to be examined. However, the test requires a full outfit to be prepared for the test, making it unfeasible for testing flame-retardant fabric treatments early in development.

Prior to scaling fabrics to the sample sizes required in the Vertical Flame test and the Mannequin test, novel treatments are screened using quantitative bench-scale tests. The aim of these bench-scale tests are to use their quantitative data to provide insight on the performance of the fabrics in the certification tests. The fabrics that exhibit favorable flaming characteristics are then scaled up, significantly reducing the cost of testing. Two of the most important tests for determining material flammability parameters of fabrics include the Cone Calorimetry and Microscale Combustion Calorimetry [8-13]. A novel method for determining material flammability of polymers and screening flame retardants is the Milligram-scale Flame Calorimeter [14-17]. The Milligram-scale Flame Calorimeter has not yet been used to test fabric flammability parameters or flame-retardant fabric treatment effectiveness, though it has provided similar results in flammability parameters and flame-retardant effectiveness as the Cone Calorimeter when using pure polymeric samples (in powder or disc form).

1.2 Bench Scale Flammability Test Methods for Fabrics

1.2.1 Oxygen Consumption Calorimetry

The Cone Calorimeter, Microscale Combustion Calorimeter, and Milligram-scale Flame Calorimeter all use oxygen consumption calorimetry to calculate the Heat Release Rate (HRR) and Heat of Combustion (HOC) for their samples. Oxygen consumption calorimetry relies on the Huggett's observations that the HRR per gram

of consumed O₂ is 13.1 ± 0.6 kJ/g-O₂ for most polymeric fuels [18]. The use of oxygen consumption calorimetry for these three bench-scale test methods justifies the comparison of HRR and HOC data among the 3 techniques. The differences in how the tests are run can lead to deviations in their HRR and HOC values.

1.2.2 Cone Calorimeter

The Cone Calorimeter is one of the most well-known and widely used bench scale tests for characterizing material ignition and flammability properties [19]. A 100 mm by 100 mm sample, up to 50 mm thick, is exposed to a conical radiant heater which provides an incident heat flux on the sample surface ranging from 0 to 110 kW/m². A 10 kV spark igniter is held over the sample until ignition is observed. The combustion exhaust is sampled and the oxygen consumed by the combustion process is calculated by measuring the oxygen concentration in the exhaust, and the mass flowrate through the exhaust. Huggett's principle is applied to calculate the time-variable HRR, peak Heat Release Rate (pHRR), and average Heat Release Rate (aHRR). A mass balance beneath the sample provides average and instantaneous mass loss rate (aMLR, MLR) and char yield. Integrating the total energy released during the test and dividing by the total mass loss provides the HOC per unit mass of the sample. Which units are used to describe HOC are decided by the user. The total energy released can also be normalized by the sample area exposed to the heat flux. Multiple tests of the same material at varying heat fluxes can be used to determine the critical heat flux for ignition (Q''_{crit}) and the ignition temperature (T_{ign}). A helium-neon laser in the gas duct provides transmittance of light through the smoke, which can be used to find the extinction

coefficient for the smoke of the material (k) using the Beers-Lambert law [20]. Figure 1.1 shows the design of the Cone Calorimeter.

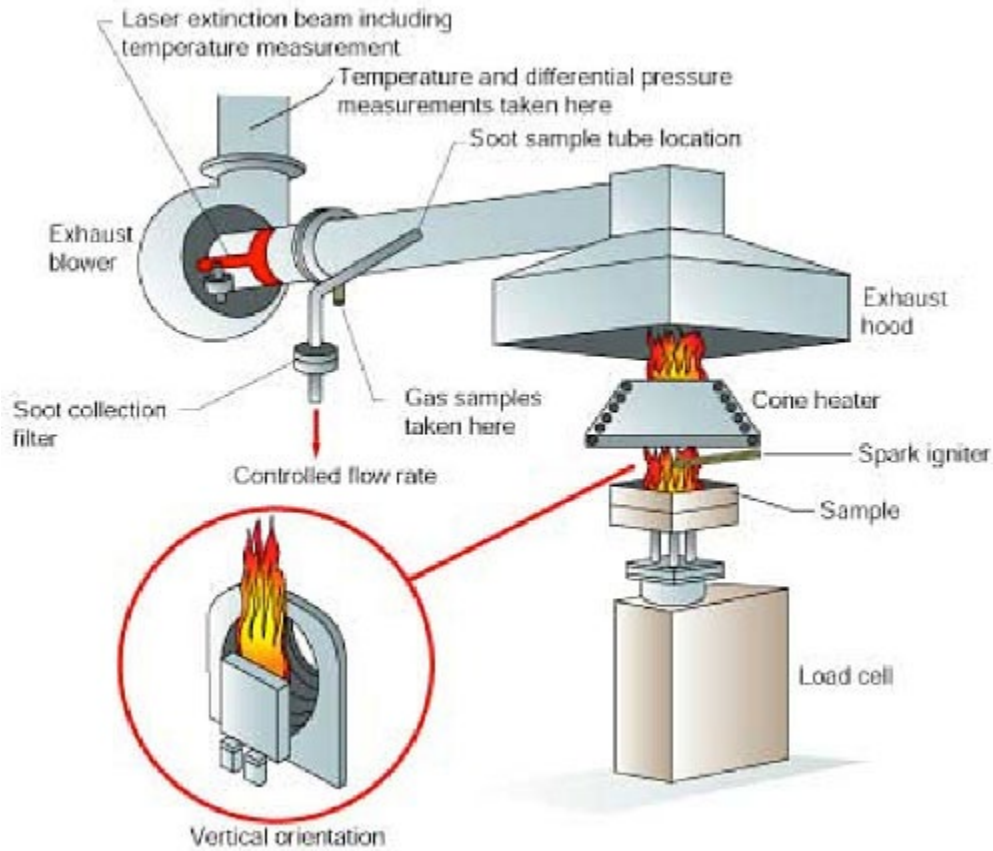


Figure 1.1: Cone Calorimeter Design Summary [21]

With over 300 devices in use worldwide [14], the Cone Calorimeter is one of the most common tools for bench-scale fire tests. It has been used to find decomposition and flaming characteristics for plastics, wood, flame retardants, fabrics, and other polymers. Certain models of the Cone Calorimeter include a controlled atmosphere, allowing for testing of materials in under-ventilated environments [22].

There are limitations to materials that can be tested by the Cone Calorimeter. Materials that undergo explosive spalling, materials that drip out of the holder

(typically only a concern for the vertical version of the test), and materials that expand into the igniter produce complications. The test assumes that the sample is thermally thick [17] which produces complications when calculating T_{ign} and Q''_{crit} for fabrics, paints and similarly thin subjects. Despite being a bench-scale test, cone samples are on the order of grams-10s of grams. This order of magnitude may be cost prohibitive for testing certain samples where only small amounts of flame-retardant treatment have been synthesized. The visualization of the condensed-phase activity of the sample is often limited by the position of the Cone above the sample and the optical depth of the flame front.

1.2.3 Microscale Combustion Calorimeter

The Microscale Combustion Calorimeter (MCC) is a bench scale test that provides intrinsic material properties for flammable substances using less than 10 milligrams of sample per test. Created by the Federal Aviation Administration (FAA) to screen flame retardants [24], the MCC provides the maximum HOC for a flammable material, similar to a bomb calorimeter, using oxygen consumption calorimetry. The relatively small samples required for the MCC enable testing of difficult to produce or acquire materials. The MCC has been used to screen materials early in development and find properties for modeling [8-10, 25-30].

The MCC, just like the Cone Calorimeter, uses oxygen consumption calorimetry to determine HOC and HRR of flammable samples by separating the pyrolysis and combustion processes of fire. Figure 1.2 shows a schematic diagram of the MCC as described in the ASTM standard D7309 [31]. The sample is prepared in a crucible and placed on a heating coil that heats up at a user-defined rate between 0.5 -

2 C/s. The standard provides two methods for calculating properties of the specimen: Method A and Method B. For Method A, an inert gas (typically Nitrogen) flows around the pyrolyzer and carries the volatile gasses to the combustion chamber, where sufficient oxygen and heat for complete combustion are provided. This prevents oxygen from reaching the specimen for smoldering reactions. Method B has dry air flow the volatile gasses to the combustion chamber, involving smoldering reactions at the cup. For both cases, air flow and oxygen concentration are measured throughout the test to determine the HRR. The sample is weighed before and after the test, providing char yield and, with the integrated HRR curve, the HOC by integrating the HRR curve, the HOC is obtained. Results are typically normalized by either initial sample mass or volatilized mass (defined as initial sample mass - final sample mass).

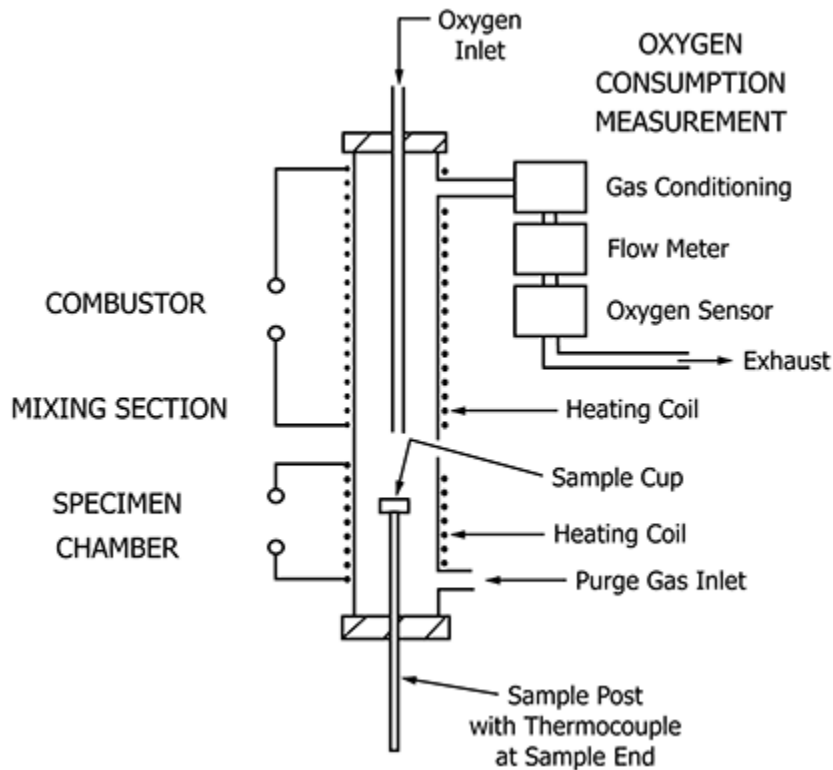


Figure 1.2: Schematic Drawing of Microscale Combustion Calorimeter (MCC) [31]

While an important bench-scale test for low-mass samples, there are some limitations on the data that the MCC can provide. The MCC's combustion chamber, at on-design operation, forces the volatile gasses to complete combustion, thus maximizing the energy release of the volatilized fuel. This complete combustion prevents soot production of the specimen and implies that the HOC measured by the MCC is the upper limit of the material being tested. Forcing complete combustion also prevents the action of several gas-phase flame retardant mechanisms. The MCC is a plug-flow combustion reactor and does not produce a flame. This combustion method prevents the observation of flame characteristics, such as smoke point, flame height, etc. The visualization of condensed-phase processes in the sample is equally impaired, as MCC samples are enclosed in an opaque pyrolyzer throughout the experiment.

1.2.4 Milligram-Scale Flame Calorimeter

The Milligram-Scale Flame Calorimeter (MFC) is a bench scale test used to find the pHRR, HOC, HRR, and char yield of samples between 30 – 50 mg through oxygen consumption calorimetry and a non-linear heating ramp through thermal conduction. The MFC was originally created to screen flame retardants at a smaller scale than the Cone Calorimeter without the limitations the MCC has in gas-phase analysis [14-16]. The MFC has undergone several updates to its design over the past decade, with the most recent updates to the pyrolyzer setup by De Beer et al. [17]. A schematic of the most recent version of MFC (prior to the current work) is shown in Figure 1.3.

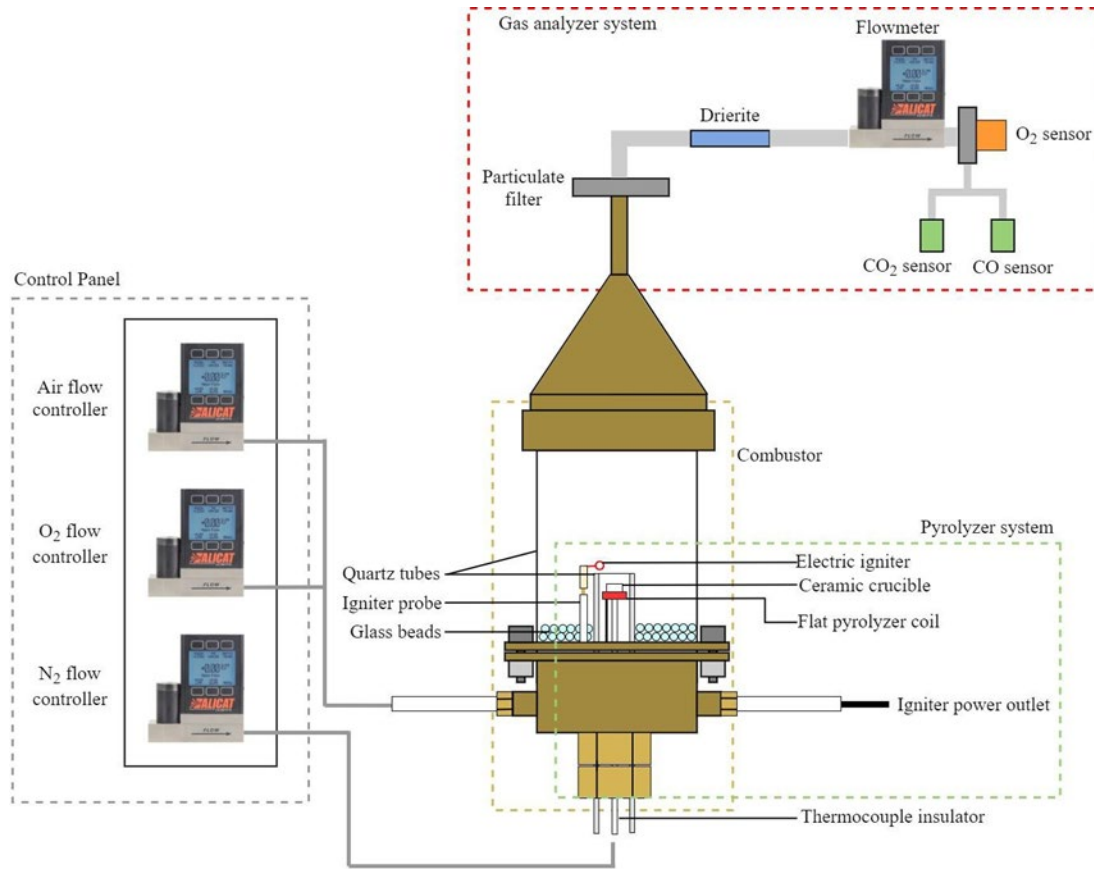


Figure 1.3: Schematic Diagram of the MFC and its Major Systems [17]

The MFC uses oxygen consumption calorimetry, similar to the MCC and Cone Calorimeter, to determine HRR and HOC for materials. In its most recent iteration, an 8 mm outer diameter (OD) 4.5 mm tall ceramic crucible is placed on top of an 11 mm OD ceramic plate with a thermocouple bead on top of the plate. A NiCr wire coil is wrapped within the ceramic plate and connected to a DC power controller, creating a hot plate. The crucible and hot plate sit on an inner quartz tube with an OD of 13.7 mm which is housed within an outer quartz tube with an OD of 75 mm. An Alicat MC-5SLPM-D/5M flow controller provides 4 SLPM of dry air through the outer quartz tube while an Alicat MC-500SCCM-D/5M flow controller provides 100 SCCM of N₂ through the inner quartz tube. The hot plate undergoes two non-linear heating ramps,

dictated by constant power settings. The hot plate pyrolyzer undergoes 2 sequential heating profiles. First the sample is heated to a steady temperature of 47 C in order to precondition the sample and to guarantee that, for any test, all samples begin their pyrolysis phase at the same initial temperature regardless of laboratory conditions. Once the sample has reached the conditioning temperature, the pyrolysis ramp rapidly increases the sample temperature, reaching a final value of 695 C. The non-linearity of the pyrolysis ramp mimics the heating profile of samples in Cone Calorimetry, and both MFC and Cone heating profiles are different from the linear profile used in MCC. Figure 1.4 shows the temperature of the pyrolyzer throughout each heating ramp. As the sample pyrolyzes, the volatile gases are pushed by the nitrogen flow through the opening of the inner quartz tube and into the air atmosphere, establishing a laminar, axisymmetric, diffusion flame. The air co-flow carries the products of combustion downstream through a 2-micron filter, capturing solid and liquid matter in the combustion products. The gases continue to flow through 1/4" tube filled with a desiccant, removing most of the moisture from the flow. The remaining gases pass through a flowmeter and a variety of sensors (one each for oxygen, carbon dioxide, and carbon monoxide).

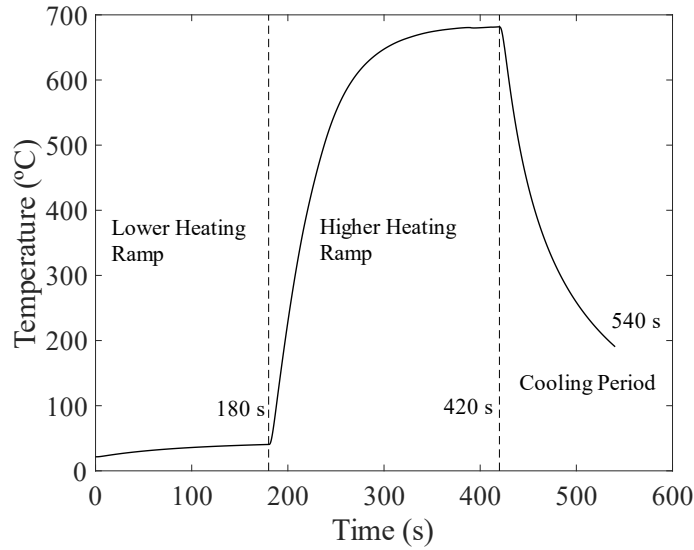


Figure 1.4: Pyrolyzer temperature during the typical MFC experiment

As the MFC uses a closed environment, the flow of gases into and out of the apparatus is known. Flow controllers upstream of the combustion chamber provide flowrate of dry air and Nitrogen in known concentrations and densities into the system, while a flow meter downstream of the combustion chamber provides the total flowrate out of the system. An electrochemical oxygen sensor (Teledyne R17a), and Nondispersive Infrared (NDIR) CO and CO₂ sensors (Edinburgh Sensors Gascard) provide the concentration of their respective gases downstream of the combustion chamber. Mass conservation is applied to the system using the following equation:

$$\Delta\dot{m}_{O_2} = (\dot{m}_{O_2})_{IN} - (\dot{m}_{O_2})_{OUT} \quad (1)$$

Where $\Delta\dot{m}_{O_2}$, $(\dot{m}_{O_2})_{IN}$, and $(\dot{m}_{O_2})_{OUT}$ are the net mass flow, the mass flow out, and the mass flow of oxygen into the system (kg/s), respectively.

Two methods for calculating the mass flow of oxygen (and therefore HRR) are used in the MFC: Method A and Method B. For Method A, it is assumed that the flowrate of oxygen into the MFC is assumed to be constant throughout the test and is

defined as the flowrate of oxygen measured in the exhaust prior to the start of the test. The difference between the mass flowrate of oxygen in and out of the MFC is calculated using the following equation:

$$\Delta \dot{m}_{O_2} = \rho_{O_2} \dot{V}_{IN} [O_2]_{IN} - \rho_{O_2} \dot{V}_{OUT} [O_2]_{OUT} \quad (2)$$

Where ρ_{O_2} is the density of air (kg/m^3) at 25 °C and 1.01 bar, \dot{V} is the instantaneous volumetric flowrate of air ($\text{m}^3/\text{kg}\cdot\text{s}$), and $[O_2]$ is the volumetric concentration of oxygen. The volumetric flowrate and oxygen concentration leaving the MFC is time-dependent, while the flowrate and concentration entering the MFC are held constant. As the flame causes pressure fluctuations within the system, the volumetric flowrate downstream of the combustion chamber can vary from the flowrate in. This can cause the instantaneous HRR to be negative at the beginning of combustion, followed by a peak HRR likely much larger than the flame can produce.

Method B uses less physically accurate assumptions to produce a HRR curve that doesn't include negative values. Method B's assumption is that the instantaneous volumetric flowrate out of the system (measured) is the same as the flowrate into the system (controlled but not measured). This allows for the net mass change to be calculated using the oxygen concentrations using the following equation:

$$\Delta \dot{m}_{O_2} = \rho_{O_2} \dot{V}_{OUT} ([O_2]_{IN} - [O_2]_{OUT}) \quad (3)$$

Where the volumetric oxygen concentration into the system, $[O_2]_{IN}$, is assumed to be constant.

MFC tests provides material properties related to fire growth and size similar to the Cone and MCC. The oxygen consumption calorimetry described above provides HRR and pHRR. Measurements of the sample mass before and after the tests provide

char yield and, along with the HRR curve, HOC. The sudden decrease in oxygen concentration caused by ignition, supplemented by visual observation and recording of the flame, provides ignition time (t_{ign}). The thermocouple on the pyrolyzer plate provides the temperature of the sample over time, yielding both T_{ign} and pHRR temperature. The paper filter is measured before and after testing to calculate the soot yield. The transparent quartz tubes allow for a high level of optical access to the sample, which may allow for qualitative analysis of the condensed-phase activity of the sample throughout the experiment.

The MFC has its own limitations. Samples that intumesce, char or bubble out of the crucible can either breach the top of the inner quartz tube and become exposed to air or spill on to the pyrolyzer. Samples need to fit within the crucible and weigh between 30-50 mg, limiting especially low-density materials. The ceramic pyrolyzer stand and hot plate are fragile and custom-made. A broken pyrolyzer requires a full replacement involving 3-4 days of building, curing and calibration.

1.3 Flame Behavior and Flame-Retardant Fabric Treatment Background

A summary of fire burning behavior is important for discussing how flame retardants decrease ignition likelihood, flame size and growth. This section will focus on the combustion of solid fuels as they are the most relevant to this current study. Solid fuel combustion exists either as a gas-phase flaming reaction or a solid-phase smoldering reaction. For flaming combustion, heat is applied to a solid fuel until it either pyrolyzes (chemically decomposes into volatile gases), sublimates, or melts and then evaporates. The gaseous fuel mixes with an oxidizer, typically oxygen in ambient air, and, in the presence of an ignition source, produces a self-sustaining diffusion

flame. Fire requires four components to be self-sustaining: fuel, oxidizer, heat, and a chemical chain reaction. These four components, often referred to as the fire tetrahedron [32], must all be present for sustained flaming. If heat is removed from the system, the global reaction rate decreases, and the fire will fail to propagate when the reaction rate falls below the diffusion rate. If not enough fuel or oxidizer is provided to the system, then the heat produced by the reaction is diluted into the excess oxidizer or fuel, lowering the temperature and reaction rate. If the chemical chain reaction is inhibited by the removal of radical molecules, then the flame will extinguish [33].

For solid fuels, flame retardants can act in either the condensed-phase, the gas-phase, or both by impeding one or more of the fire tetrahedron components. In the condensed-phase, flame retardants can increase the charring rate of the material, decreasing the production of volatiles and providing insulation between unburnt fuel and the heat source [34]. Intumescent flame retardants decompose before the material beneath it, forming a thick, thermally stable char layer to insulate the flammable polymer [35]. Endothermic flame retardants absorb heat, reducing the temperature of the polymer and volatile production [36].

Gas-phase flame retardancy involves the decomposition of the flame retardant into a gas that impacts the flame directly. Some gasses only dilute the flames, both absorbing heat and reducing the concentration of fuel and oxidizer [34]. Others can react with the radical molecules in the flame front to impede chain-branching reactions and extinguish or suppress the flame. The chemical interactions of flame retardants try to reduce the production of heat and radicals by either combining with radicals to

produce relatively unreactive molecules or recombining the radicals into their previous states [36].

The MFC, MCC and Cone Calorimeter provide information on the material properties of combustible materials that can help researchers observe the effectiveness of the flame retardants. Onset of ignition (either T_{ign} or t_{ign}) help inform if and when a material will begin to ignite. Char yield provides information on the production and thermal stability of the char. pHRR is related to both flame length and flame spread, with lower pHRR decreasing both [37]. HOC for the gasified mass of a material informs the total heat produced by the flame, while HOC for the initial mass relates to the total fuel load of the material. Comparison of these properties against each other, alongside visual observation during and after the tests, is critical to interpreting the flame-retardant mechanism.

There are often negative externalities when using flame retarded materials. For fabrics, flame retardants apply an additional mass to the untreated fabric, making it more costly to transport and use. Halogen-based flame retardants are often so chemically stable that they can accumulate in humans and animals; a significant environmental and public health issue [38]. Flame retardants can also reduce the positive mechanical properties of the fabric, making them less comfortable, durable, or tear-resistant [39]. Producing and applying flame retardants to fabrics adds additional overall costs, which quickly add up when produced at the scale of military uniforms. These factors drive current and future research in flame retardants to make products that are safe and effective.

1.4 *Objectives*

Both the Cone Calorimeter and the MCC have certain drawbacks when testing flame retardant fabric treatments. For the Cone, the sample size for a single test can be prohibitively expensive for screening flame retardants during the early R&D phases. Samples that drip or significantly intumesce can also provide additional complications and attention. For the MCC, because it forces combustion to completion, gas-phase interactions are often lost [25].

The MFC was created to address most of the aforementioned drawbacks and has been used in the past to detect both gas-phase and condensed-phase flame retardant activity [15]. While previous versions of the MFC could only test granulated powder or shavings of materials [14] and had difficulties with highly charring materials, updates to the design by De Beer et al. [17] allow for larger and intumescent samples to be tested. These recent updates open up the MFC to potentially testing fabrics, as a layer of fabric can now lay flat against the crucible. The smaller sample sizes used by the MFC make it economically viable to test materials early in development.

Despite these advantages, the MFC has yet to be used to test fabrics, and the unique features of fabric samples may pose certain challenges with testing. The low density-to-area ratio of fabrics means that they might not produce enough volatiles for flaming combustion, especially when flame retardants are applied. Taking the advantages of the MFC and the challenges of fabric testing into consideration, the objectives of this work are twofold:

- 1) Investigate the feasibility of testing fabric samples in MFC, including modifications to the apparatus and an exploration of optimum sample preparation.
- 2) Use the improved testing methodology to investigate the MFCs capability to detect flame retardant activity using 2 common fabrics (Cotton and Nylon).

These results will be compared with MCC and Cone Calorimeter data to benchmark the MFC against these well-known bench-scale methods. Additionally, this current work is part of the larger HEROES research project investigating new flame-retardant fabric treatments for United States military uniforms. The military uniforms are composed primarily of 50% Nylon 50% Cotton blends (Nyco). The outfits need to pass Department of Defense (DOD) standards related to the Vertical Flame Test and Mannequin Flame Test. Part of the research includes using bench-scale, quantitative combustion tests, including the Cone and MCC, to predict the likelihood of a flame-retardant fabric treatment to pass or fail the DOD requirements. Alongside the other objectives of this study, the potential for the MFC to provide quantitative or qualitative data that may be useful in helping predict a fabric's success in the Vertical Flame Test will be examined and discussed.

2 Updates to Milligram-scale Flame Calorimeter Design

The current work provided an opportunity to improve on the prior MFC design to address uncertainties in the performance of certain components, user experience, as well as the ability of the apparatus to handle fabric samples. This chapter will discuss the updates and modifications to the MFC in the context of the current work.

2.1 *Igniter Power Supply*

To increase user control and repeatability of the igniter system, a new power supply was introduced for the MFC igniter coil. The previous system used a dial voltage controller, with the igniter set to 10% of the maximum voltage when operational. This required qualitative judgement on the brightness of the igniter, took a few seconds to properly adjust, and could lead to melting of the igniter wire if the power was increased too high. A programmable power supply provides a more precise control over the igniter, as the voltage and current flowing through the wire are visually displayed on the device in real time. The NANDKAF 30V-10A Programmable DC Power Supply provides a digital readout of voltage, current, and total power in the igniter system. The digital power readout allows for the igniter power to be kept at $50 \text{ W} \pm 1 \text{ W}$ during experiments, with a 2 second delay time for start-up and cool down. The programmable power supply is more precise than the previous system, activates with a single button press rather than adjusting a knob, and prevents the igniter from melting or permanently deforming during MFC tests. In addition to the new power supply, fresh igniter coils were produced using the same design as De Beer's previous work [29].

To characterize the precision of the new power supply and new igniter coils being used, tests were performed to determine repeatability of the igniter. Figure 2.1 shows the temperature increase of the heating plate by itself from 1-minute exposures of the igniter in normal flow circumstances. Error bars for this figure and all subsequent figures were calculated with the following equation,

$$Error = \frac{A_{max} - A_{min}}{2}, \quad (4)$$

Where A is the parameter being evaluated in the graph. This error method was used as all tests were run in triplicate for each unique sample or method used. The new power supply provides a high level of precision, as the error between tests does not exceed ± 1 W. The hot plate temperature increasing at such a significant rate, however, brought attention to its current use. De Beer's thesis on the previous updates to the MFC denotes that the igniter was turned off 5 seconds after sustained flaming is observed [17]. The thesis also asserts that during the high heating rate, the heat applied by the igniter to the specimen is proportionally much smaller than the heat applied by the pyrolyzer plate.

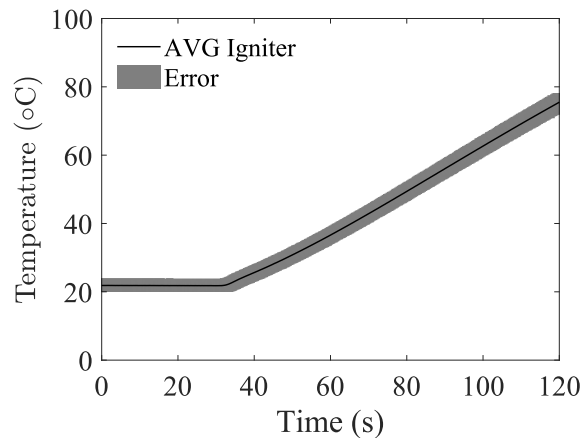


Figure 2.1: Igniter Power Captured by Temperature Increase in Pyrolyzer

To resolve the inconsistency between the findings in Figure 2.1 and De Beer's thesis, tests were run to compare the temperature of the heating plate during the high heating ramp with and without the igniter. Figure 2.2 compares the temperature of the heating plate and crucible with and without 1 minute of the igniter operating during the high heating rate to investigate the proportional heating assertion. Note that for both this graph and all future graphs, marker placement is arbitrary and does not represent frequency of measurements. Markers are placed every 10 data points, except for Cone tests where markers are every 3 data points. The heating rate of the sample does increase, somewhat slightly, with the igniter coil running. It was also observed that turning the igniter off 5 seconds after self-sustained ignition began was difficult to track for smaller flame, such as cotton, and highly turbulent, flashing flames, such as nylon. The new methodology turns the igniter off 50 seconds after the beginning of the high heating rate, which is enough time to ensure self-sustaining ignition for the control Nylon.

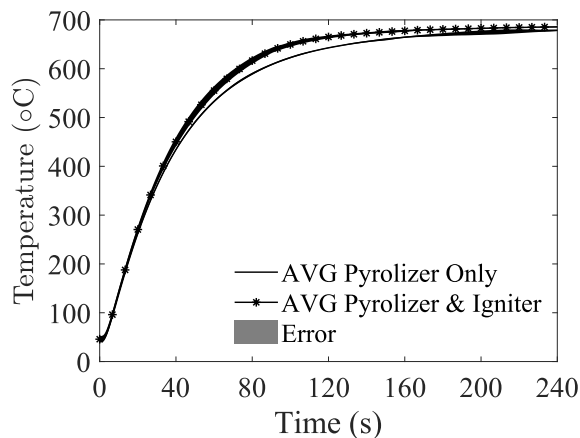


Figure 2.2: Pyrolyzer Temperature with and without Igniter on during first 60 Seconds

2.2 Temperature Repeatability

Multiple new pyrolyzer stands, following the design from De Beer's previous work [17], were produced for this current study. The pyrolyzers can endure approximately 40-50 tests before they begin to exhibit signs of fatigue through lower and less precise heating ramps. The previous thesis mentioned that most of the work had been done with a single pyrolyzer stand and compared the final temperatures those two pyrolyzers reach at varying voltage settings. This current study investigated the repeatability of the higher heating ramp within a single pyrolyzer and the reproducibility of that heating ramp across multiple pyrolyzers.

Figure 2.3 shows the average temperature curves between two separate pyrolyzers during the high heating rate. The original pyrolyzer was used for all other tests in this current study, while the new pyrolyzer was created for future use. The repeatability of both pyrolyzers is very high, with an error of less than 1°C throughout the heating ramp. However, the reproducibility of the pyrolyzers appears to be limited. The heating rate input voltages for the original pyrolyzer were 0.58 and 0.995 V for the lower and higher heating rates, respectively, while the input voltages for the new pyrolyzer were 0.56 and 0.945 V. A deviation in temperature is apparent through the entire Temperature curve, indicating a difference in heating rates. The peak and average heating rate for the original pyrolyzer are 11.2 K/s and 2.73 K/s, respectively, while the new pyrolyzer peak and average heating rate are 12.2 K/s and 2.67 K/s, respectively. The heating rate during a burn test can have a significant impact on the flame behavior of the material and is an important independent variable for TGA, MCC, and Cone tests [40-46].

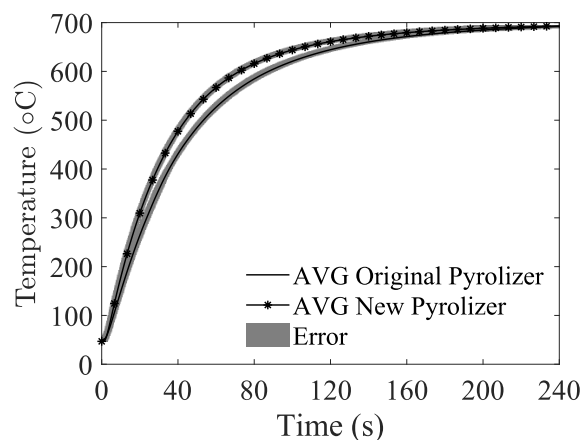


Figure 2.3: Pyrolyzer Temperature between two Pyrolyzers

Cotton tests were performed to evaluate the impact the different heating rates would have on the flame characteristics values provided by the MFC. Table 2.1 shows the HOC, T_{ign} , t_{ign} , and pHRR for the two pyrolyzers. Details on how the values provided in Table 2.1 were calculated are provided in section 3.4 and 4.3. It should be noted that not all of the differences between pyrolyzers can be accounted for by the change in temperature curves: the position of the pyrolyzer in the quartz tube, the calibration of the gas cards and flow meter, and position of the crucible on the pyrolyzer can also impact test repeatability. Regardless, the decrease in HOC and pHRR as well as the increase in T_{ign} for the new pyrolyzer is evident in table 2.1. These variations are within the 10% error inherent in using oxygen consumption calorimetry to calculate HRR and HOC [18]. Due to time constraints, methods to improve the reproducibility of the pyrolyzer are not included in this current study and will be the focus of future research.

Table 2.1: Cotton Tests using the Original Pyrolyzer (the pyrolyzer used for the other tests in the current study) and the New Pyrolyzer

	Original Pyrolyzer	New Pyrolyzer
Initial Mass (mg)	28.1 ± 1.2	28.6 ± 0.5
Char Yield (%)	0	0.5 ± 0.3
T _{ign} (°C)	381 ± 6	405 ± 11
t _{ign} (s)	37 ± 1	36 ± 2
pHRR, (W/g)	565 ± 7	511 ± 5
pHRR, (kW/m ²)	89.8 ± 0.6	81.0 ± 0.4
HOC per initial mass (kJ/g)	14.1 ± 0.4	13.3 ± 0.5
HOC per gasified mass (kJ/g)	14.1 ± 0.4	13.4 ± 0.5

2.3 *New Coupler for Glass/Cone Connection*

A new coupler was designed for the MFC to incorporate an inflatable seal between the downstream flow line and the combustion chamber quartz tube. The previous seal, a 2 7/8" ID, 3 1/8" OD nitrile O-ring didn't always fit the quartz tube due to tolerance variability between quartz tubes. It also tended to chip the quartz tube when being placed or removed. The inflatable seal design allows for easy placement of the cone on top of the quartz tube, followed by pressurizing the tube to make an air-tight seal. The neoprene inflatable seal had an OD of 87 mm, an uninflated ID of 76 mm, inflated by 1 mm. The size of the inflatable seal required a new coupler to be built. Figure 2.4 shows the schematic design for the cross section of the inflatable seal and the seal outside of the coupler.



Figure 2.4: Schematic Cross Section of the Seal (Left), Top-Down View of the Seal (Right)

Figure 2.5 shows the design for the inflatable seal system. Air from an air compressor was brought in to a regulator and maintained at 25 PSI. A three-way valve provides a setting for inflating the seal and removing the air in the seal during deflation. A 30 PSI spring-loaded relief valve acts as a safety feature in the case where the air compressor malfunctions. Initial tests with the seal showed that it would maintain an air-tight seal around the combustion chamber quartz tube as intended. However, similar issues of tolerance variability that occurred with the o-ring occurred with the inflatable seal. The 1 mm inflation distance did not consistently create a seal that prevented leaks. A larger seal and coupler are currently being designed to overcome this issue. Due to time constraints, that design wasn't ready for this current study, and a temporary silicone sealant was applied to the connection to maintain an air-tight seal for experiments performed in this current study.

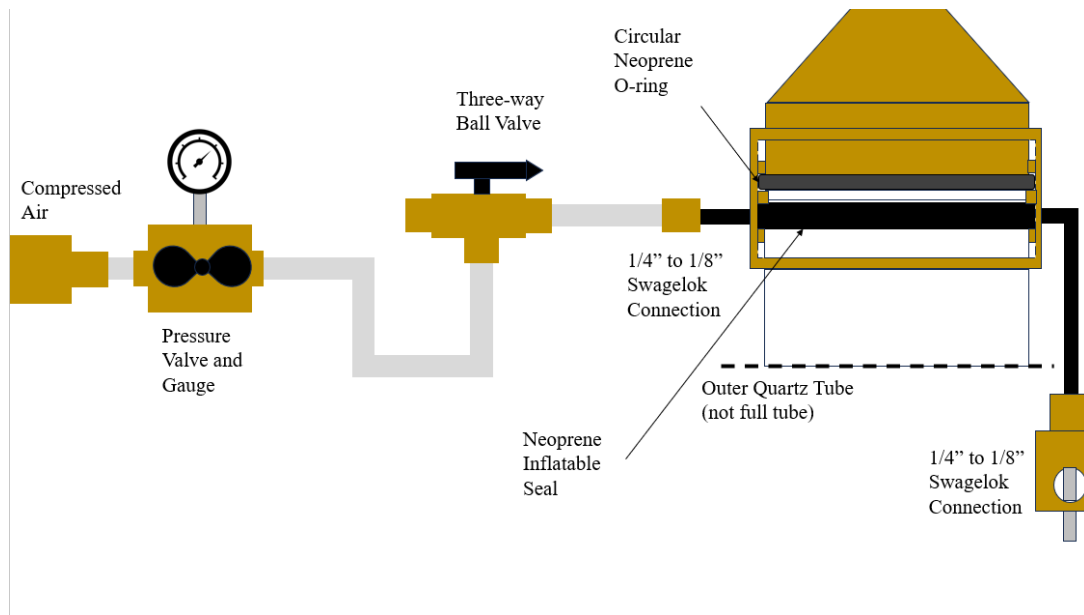


Figure 2.5: Diagram of the Inflatable Seal System

2.4 Comparison to Previous MFC data

PMMA and PVC Benchmark tests were performed using the MFC to compare against results from the most recent MFC work. PMMA and PVC (disks) were chosen as they were used in De Beer's thesis [17], PMMA produces very little char during pyrolysis, and PVC produces a considerable amount of char. Figure 2.6 shows the comparison between the average HRR curves for PMMA and PVC between the benchmark tests and De Beer's thesis. Table 2.2 shows the initial mass, t_{ign} , T_{ign} , char yield, pHRR, HOC per total sample mass, and HOC per gasified mass.

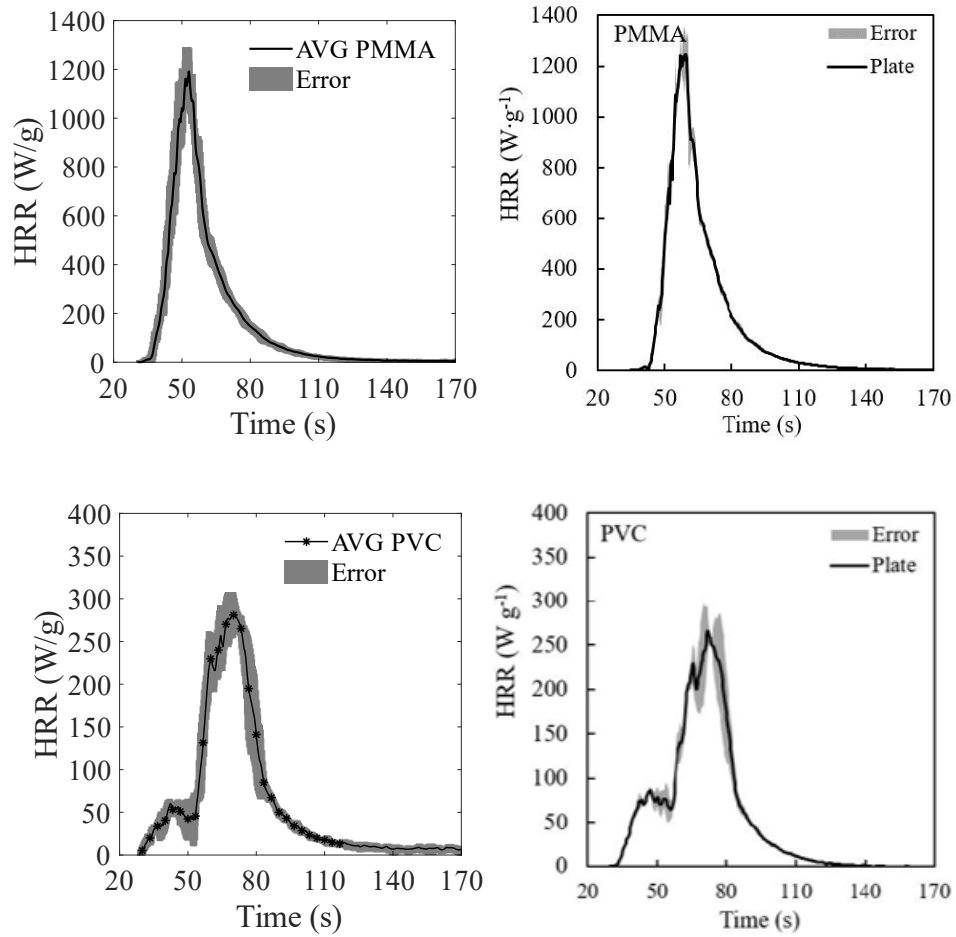


Figure 2.6: Average HRR curves for PMMA (disk) and PVC (disk) for current MFC (left) and De Beer's Results (right) [17]

Table 2.2: Current MFC results vs. De Beer's MFC Results for PMMA and PVC [17]

	New PMMA Tests	De Beer's PMMA Tests [17]	New PVC Tests	De Beer's PVC Tests [17]
Initial Mass (mg)	37.2 ± 5.8	40.0 ± 0.47	50.1 ± 1.7	57.08 ± 5.8
t_{ign} (s)	37 ± 0.5	44 ± 1.1	35 ± 0.5	38 ± 0.5
T_{ign} (°C)	383 ± 3	439 ± 11	360 ± 5	392 ± 8
Char Yield (%)	0	0.33 ± 0.09	13.5 ± 1.0	17.3 ± 2.1
pHRR (W/g)	1230 ± 50	1160 ± 30	285 ± 22	269 ± 2
HOC, Initial Mass (kJ/g)	24.3 ± 0.1	24.2 ± 0.7	$8.66 \pm$ 0.22	7.42 ± 0.48
HOC, Gassified Mass (kJ/g)	24.3 ± 0.1	24.3 ± 0.7	10 ± 0.26	9.27 ± 0.21

While the HRR curves show similar shapes for the current and previous tests, the t_{ign} and T_{ign} for both PMMA and PVC were lower in the current study's tests than De Beer's thesis [17]. The t_{ign} for the current and previous MFC tests follow a similar trend. It is possible that the igniter was placed closer to the top of the crucible in the current study's tests, leading to an increase in temperature on the top of the sample. This thermally thick sample would insulate the thermocouple on the bottom of the crucible from the igniter's heat, leading to a lower recorded T_{ign} . It's also possible that while the current MFC pyrolyzer reaches a similar asymptotic temperature as the previous MFC update, the heating rate to that asymptote may differ. A slower heating rate would decrease thermal lag between the pyrolyzer and the sample, leading to a lower T_{ign} .

Char yield and HOC were also higher for the benchmark tests compared to the De Beer's tests [17]. The crucible lies in a pure Nitrogen flow to prevent smoldering and carry the volatile gasses out of the inner quartz tube. However, the residue from preliminary cotton tests was a ball of ash rather than char, indicating the presence of oxygen in the inner quartz tube. The decrease in char yield between the benchmark tests and De Beer's tests, especially for PVC, provides additional evidence for this theory. Tests with a full Nitrogen purge (Nitrogen flow in both the inner and outer quartz tubes) were conducted with PVC, providing similar char yields to De Beer's work. The current theory is that the current pyrolyzer stand is positioned to produce an uneven flow in the inner quartz tube, leading to turbulence that entrains air into the crucible. The decrease in char likely led to the increase in HOC for the PVC benchmark tests. This theory could also explain the reduced t_{ign} and T_{ign} of the check tests. The concentration of volatiles are highest at the surface of the sample, decreasing with height. Entrainment of air closer to the fuel source can initiate combustion earlier or lead to oxidative pyrolysis prior to flaming ignition. Due to time constraints, this entrainment issue is still being investigated and will be the study for future research.

3 Experimental Design

As the MFC has not yet been used for testing the flaming characteristics of fabrics, a detailed discussion on how and why the samples were prepared is merited. This section will discuss the details on the fabrics and flame retardants used and the methodologies for each test setup, including how samples were prepared.

3.1 Fabric Origins and Flame-Retardant Application

The fabrics tested for this current study include Cotton, Nylon 6,6, Cotton with 20% weight gain of Phosphoric Acid (PA), and Nylon with 9% weight gain Tannic Acid (TA). The longer-term goal for this research is to understand and characterize flame retardant treatments for Nyco. However, as the MFC has not previously been used for testing fabrics, a better starting point would be to examine combustion properties for Cotton, Nylon, and a single flame retardant for each control fabric. This set of tests allows for both comparison between fabrics that vary significantly in burning behavior and how that burning behavior changes from control fabric to flame-retardant treated fabric. For the rest of the current study, Cotton Control refers to the untreated Cotton, while Nylon Control refers to the untreated Nylon.

All fabric samples were initially prepared by Kulkarni and Nagarajan of the University of Massachusetts, Lowell. Details on the origins of the fabrics and the chemicals used for flame retardation and the application of those flame retardants can be found in their previous work [47].

For all fabric samples, the preparation began with boiling the fabrics in deionized water for 1 hour to remove foreign particles. The fabrics were then dried in

a forced convection hot air oven at 80°C for 12 hours to remove any moisture. No additional preparations were used for the control fabrics.

The Phosphoric Acid (PA) Cotton samples covalently bonded modified Phosphoric Acid to the cotton through phosphorylation. A solution of 1 mol Phosphoric Acid for 3.2 moles Urea was dissolved in deionized water at a liquid ratio of 1:1.5. This solution contained 5% Phosphorous (element) by mass. The cotton was soaked in the solution, then air dried for 30 minutes. The PA Cotton was then dried in a forced convection hot air oven at 155°C for 45 minutes. The fabric was then washed in deionized water at 60°C for 15 minutes twice. The areal density for the PA Cotton samples was 188 g/m².

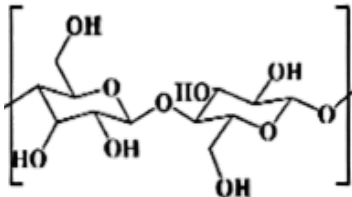
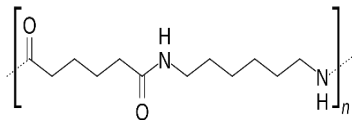
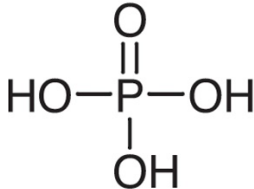
The Tannic Acid (TA) was applied to the Nylon samples through a mordant dyeing technique. 20% on mass of fabric (omf) was dissolved in a deionized water solution with a liquid ratio of 1:40. The pH of the solution was measured and maintained between 3 and 3.5, using acetic acid (reagent plus grade, Sigma Aldrich) to lower the pH when necessary. The Nylon was boiled in the solution for 1 hour. After cooling to room temperature, the TA Nylon was washed in deionized water at 60°C for 15 minutes twice. The areal density for the TA Nylon samples was 243 g/m².

These samples were delivered to the University of Maryland in 2" x 4" fabric strips. In the original work by Kulkarni et al. [47], Phytic Acid was used as the flame retardant for cotton. Due to contamination issues, Phosphoric Acid was used in place for the samples in the current work.

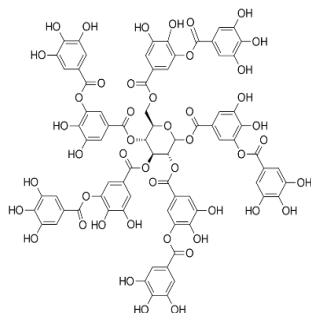
Table 3.1 provides the Structure and background information on the polymers and flame retardants tested, while Figure 3.1 shows the chemical structure of the fabrics

with flame retardants attached. The Urea and Phosphoric Acid combined to replace two of the OH branches of the acid with $O^-NH_4^+$. The modified PA is covalently bonded with the Cotton cellulose, while the TA creates a hydrogen bond with the Nylon 6,6.

Table 3.1: Fabric and Flame Retardant Chemical Line Structures and Other Info

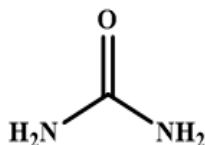
Polymer/Flame Retardant	Repeat Unit	Additional Information
Cotton		Plain Weave, Undyed, 156 g/m ² , Test Fabric (Pennsylvania, USA)
Nylon 6,6		Plain weave, Undyed, 500 Denier, 100%, Brittany Global Technologies 212 g/m ² (Massachusetts, USA)
Phosphoric Acid		ACS Grade, Sigma Aldrich

Tannic Acid



ACS Grade, Sigma Aldrich

Urea



ACS Grade, Fisher

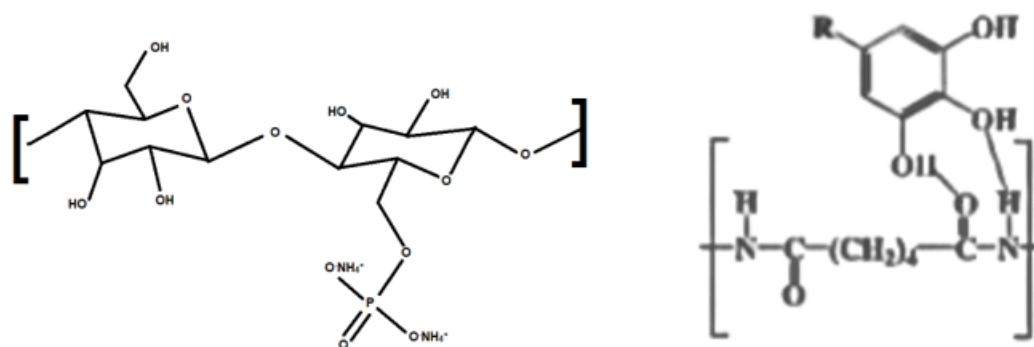


Figure 3.1: Chemical Structure of the Cotton with Phosphoric Flame Retardant and Nylon with Tannic Flame Retardant

3.2 *Cone Calorimetry Methodology*

3.2.1 Cone Calorimeter Setup

Cone Calorimetry tests were run by Dr. Alexander Morgan at the University of Dayton Research Institute using the CC-2 by Deatak (McHenry Illinois, USA). Tests were run in accordance with ASTM E-1354 [19]. The fabrics were cut into 100 x 100 mm square samples. A wire grid made of 2 mm nominal stainless-steel rods with 18

mm x 18 mm openings was placed on top of the sample. 0.02 mm thick Foodservice grade aluminum foil was wrapped around the bottom, sides, and approximately 2 mm over the top of the sample. A piece of 13 mm thick ceramic fiber insulation was placed underneath the foil. The board and foil were placed in a 1.9 mm thick stainless steel mount assembly of 111 mm x 111 mm x 54 mm dimensions. The edge frame of the mount reduces the exposed area of the sample to 88.4 mm². Due to observed sample behavior under heat exposure, the area of the mesh is not accounted for in this reduction. All samples were run at an exhaust rate of 24 L/s and 50 kW/m² heat flux. Tests were run in triplicate for each fabric material. Data was recorded at 1/3rd Hz. Additional details on deviations from the standard can be found in Morgan's report [48].

3.2.2 Cone Calorimeter Post-Processing

The raw HRR data was used to create HRR curves over time and determine peak and average HRR. Raw HRR was normalized by the exposed area of the sample (0.0884 m²). The t_{ign} and time to extinction (t_{ext}) were based on visual observations of when a stable flame was first observed and when it disappeared. The fabric portion of the sample was weighed before the test began and the mass balance was zeroed to match the weight of the fabric. The mass balance built into the Cone tracked the weight of the sample over time. The initial and final mass of the sample were used to calculate total mass loss and char yield. The total mass loss was used with the HRR data to calculate the HOC.

3.3 MCC Methodology

3.3.1 MCC Setup

MCC tests were performed by Dr. Alexander Morgan at the University of Dayton Research Institute using the MCC-1 by Deatak. Tests were performed in accordance with Method A of ASTM D-7309 with a 1°C/s heating rate and the combustion furnace temperature set to 900°C [31]. Fabrics were cut into circular pieces fitting within the 5 mm ID alumina crucible. A single layer of the test fabric was used for each sample. Samples weighed between 5.36 mg and 5.65 mg across all fabrics. Additional details on deviations from the standard can be found in Morgan's report [49].

3.3.2 MCC Post-Processing

The raw HRR data was used to create HRR curves over time and determine peak and average HRR. The three tests conducted for each fabric were averaged between 200 °C and 600 °C, as all fabrics decomposed within this range and the MCC maintained the 1 °C/s heating rate throughout these temperatures. The samples were weighed before and after each test, providing the initial and final mass measurements. The total mass loss was used with the HRR data to calculate the HOC. Char yield was calculated by dividing the final mass by the initial mass.

3.4 MFC Setup

Fabric samples for the MFC were cut into 7.5 mm OD disks using a 7 mm fabric hole puncher. Fabric embroidery scissors were used for additional cuts. Nitrile gloves were worn at all times when handling the fabrics. Fabrics were cut on a board of PMMA

with a thin paper lining that was cleaned before each cutting session. Fabrics were either kept in a plastic bag or on a cleaned quartz table before testing.

3.4.1 MFC Layer Depth

One of the major concerns for using the MFC for fabric testing was that the low density-to-area associated with most fabrics can make it challenging to obtain repeatable and consistent data. As flame retardant treated fabrics can exhibit considerably lower HRR than their untreated counterparts, the flames produced by untreated fabrics need to be significant enough so that a percentile decrease in HRR won't be within the margin of error. One method for overcoming this problem was using multiple layers. The height of the crucible allows for at least 4 layers of untreated Cotton or Nylon to fit within the crucible without perturbing out. While using multiple layers of a sample is much less efficient than one layer, the amount of material used for a single MFC test compared to a Cone Calorimeter test is still 2 orders of magnitude. Fabrics are typically designed to be used as a single layer, however, so using fewer layers brings the tests closer to real use cases.

Figure 3.2 shows the measured oxygen concentration for 1 layer, 2 layers, and 4 layers of untreated Cotton tested in the MFC. Cotton was used over Nylon because Cotton has a lower HOC and therefore its combustion behavior in the MFC will dictate the minimum fabric mass required. The raw oxygen concentration is presented instead of HRR because one of the major concerns for layer depth is the error range of the instruments collecting the data. Each curve shows a similar shape, indicating that the HRR curves produce similar shapes across layer counts.

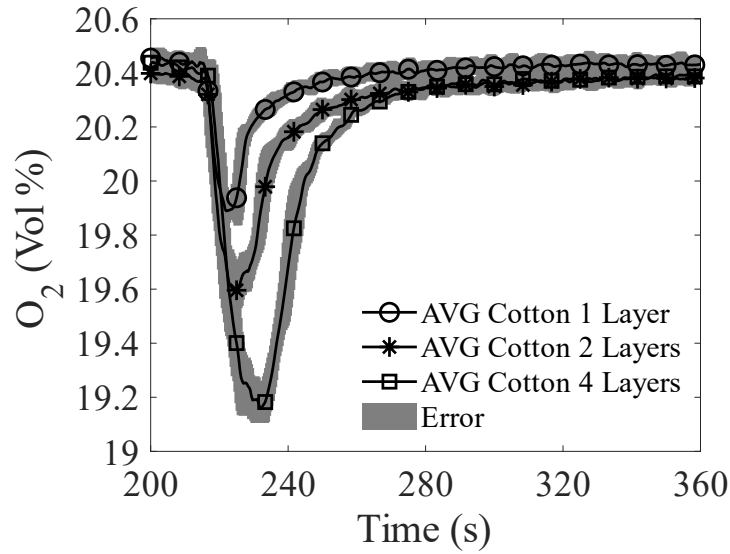


Figure 3.2: Oxygen Concentration for Burning 1 Layer, 2 Layers, and 4 Layers of Cotton

The changes in concentration from the beginning of the test to the minimum concentration determined are provided in Table 3.2. The 4-layer sample is the only layer count that decreases the oxygen concentration by at least 1 vol%. While the absolute error for 1 layer is the smallest, the relative error for 1 and 4 layers are much smaller than the 2 layer tests. Table 3.2 also shows the average mass of the samples per number of layers. Previous tests with the MFC [17] used masses between 30 – 50 mg. This range of sample masses was chosen so that tests would stay within the optimal range for the oxygen sensor. The 4-layer cotton samples are the closest of these tests to that range, providing an additional reason to use 4 layers.

Table 3.2: Maximum Change in Oxygen Concentration for Multiple Layers of Cotton

Layer Count	Concentration Decrease (vol%)	Initial Mass (mg)
1	0.54 ± 0.02	7.09 ± 0.34
2	0.77 ± 0.09	13.6 ± 0.89
4	1.27 ± 0.05	27.4 ± 0.6

Figure 3.3 shows the flames produced by the varying layers of Cotton at their peak. As the flamelets are difficult to observe, the raw video footage was post-processed to remove the igniter glare and highlight the flame. The single layer samples never produced a axisymmetric diffusion flame, only creating a localized flamelet attached to the igniter for a short time. The two layer samples produced a larger flamelet. The four-layer samples produced the largest flamelet and the closest to an axisymmetric diffusion flame. Most undesired flames that occur outside of the laboratory with fabrics will be diffusion flames, with turbulent flames for fires that consume upholstery or an entire outfit. The smaller blue flamelets act differently than larger axisymmetric diffusion flames, which can impact the flame parameters studied. For this reason, and the oxygen concentration concerns, all additional tests were run with 4 layers of fabric.

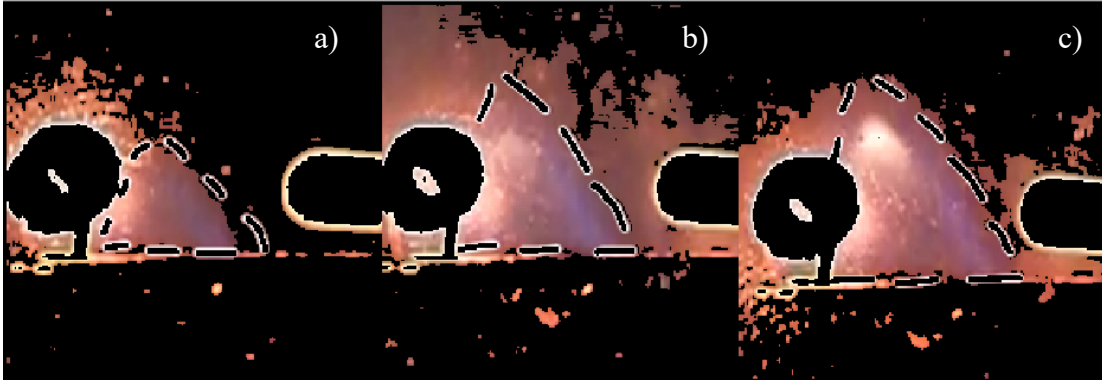


Figure 3.3: Flame Height and Behavior for 1 Layer (a), 2 Layers (b), and 4 Layers of Cotton (c)

3.4.2 MFC Sample Packing

The decision to use multiple layers of fabrics per sample provides the additional challenge of keeping the samples consistently packed together. As the heat travels from the bottom of the crucible through each layer of fabric, contact resistance plays a critical role in how quickly the sample will decompose. A mesh grid or a grated plate could lead to jets forming and increase condensate formation. Clamps on the side of the crucible might have tolerance issues when used with different crucibles. Using a metal tamper to keep the layers down wouldn't interfere during the experiment, but the packing may be inconsistent depending on the force applied by the researcher. A ring that fits around the sides of the crucible would be easily repeatable but might not keep the fabric surface even.

Two separate methods for packing the samples were investigated: the Tamper method and the Ring method. For the Tamper Method, the fabric was cut into 7 mm OD circles using a fabric hole puncher. Fabric shapes were adjusted using a pair of embroidery scissors. Each layer of fabric was placed on top of the crucible and then

tamped down with a metal tamper. For the Ring Method, the previous steps were also followed, with the addition of a 6.5 mm OD copper ring pushed down on top of the fabric layers. Figure 3.4 shows a crucible loaded with 4 layers of cotton with and without the metal ring. It is difficult to tell how well packed the Tamper method sample is, while the Ring method sample appears to bulge in the center.



Figure 3.4: 4 Layers of Cotton packed into the crucible with the Ring Method (Left) and the Tamper Method (Right)

Two sets of three tests were run for cotton using both the Tamper method and the Ring method to determine which method had the highest precision. Figure 3.5 shows the HRR for 3 tests of each packing method, while Figure 3.6 shows the error in HRR between the two sets of tests. The Ring method appears to cause the ignition time to increase and deviate more than the Tamper method. As the ring weighs approximately 240 mg, the increase in ignition time is likely due to the increased heat capacity that the metal adds to the crucible. Any similar devices used to keep the fabric well-packed during the experiment are likely to cause similar issues. The decrease in precision is observable, though a full understanding of the physical mechanism

responsible for the observation would require additional testing. It is possible that the bevel seen in Figure 3.6 for the Ring method disrupts the heat transfer through the layers. Similar to the Tamper method, there was no way to gauge how much force was applied to the Ring when packing it into the sample. It is possible that the Ring method causes similar discrepancies in packing thickness as the Tamper method, but to a larger degree. Regardless, the Tamper method is used for all future fabric experiments discussed within this current study, as the precision of the tamper method was evidently the superior of the two methods.

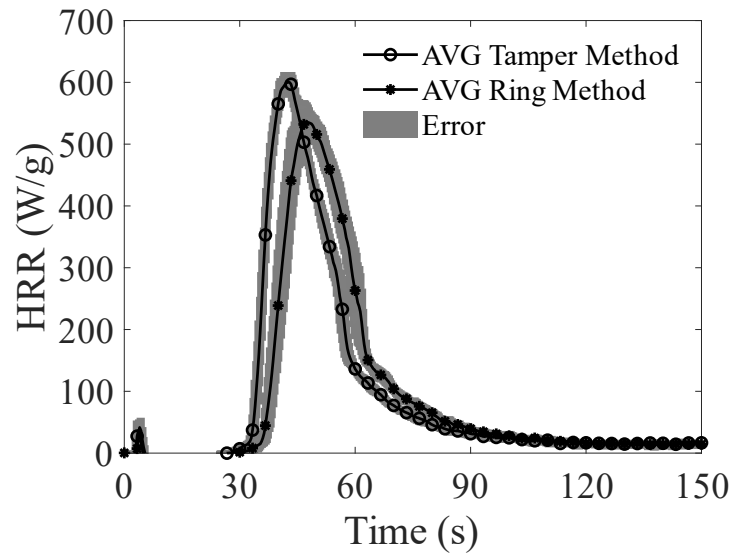


Figure 3.5: HRR for 4 Layers of Cotton with the Tamper Method and the Ring Method

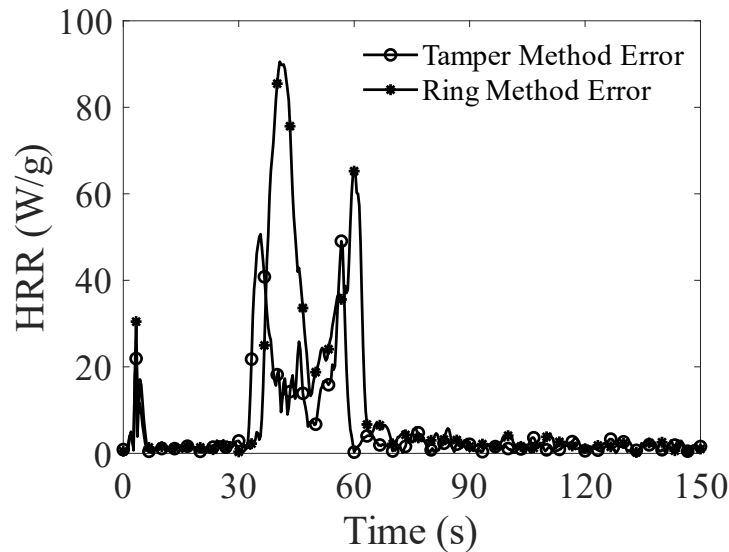


Figure 3.6: Error in HRR for 4 Layers of Cotton with the Tamper Method and the Ring Method

3.4.3 MFC Setup Information

MFC samples were prepared based on the preliminary fabric testing discussed in section 2. 3 tests were conducted for Control Cotton, Control Nylon, PA Cotton, and TA Nylon. The fabrics were cut into 7 mm OD circles and tamped into an alumina crucible. Figure 3.7 shows examples of a single layer for each fabric cut to fit within the MFC crucibles. The crucible was weighed on a laboratory microbalance (A&D weighing, BM-22) before loading the sample, after loading the sample, and after the test concluded. These measurements provide the initial mass of the sample and are used to calculate char yield. Two cameras were set up to record the samples: a camera set level with the top of the crucible to record gas-phase activity and set above the sample at a 45° angle with the sample to record condensed-phase activity.

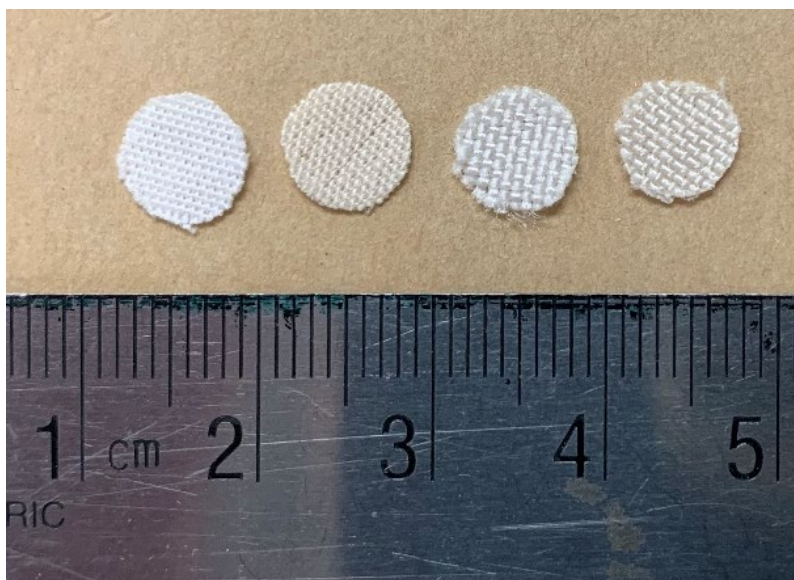


Figure 3.7: MFC Fabric Samples, (from left to right) Cotton Control, PA Cotton, Nylon Control, TA Nylon

Each MFC test begins with preparing the sample and placing it on top of the pyrolyzer plate. The combustion chamber is closed and the nitrogen and oxygen gas flow controllers are set to the flow rates described in section 1.2.4. Data collection begins when the lower heating ramp, a non-linear increase in the pyrolyzer plate to 47°C over 180 seconds, begins. The camera parallel with the top of the crucible begins recording 60 seconds after the start of data collection. At the end of the lower heating ramp, the higher heating ramp, a non-linear increase to 695 °C over 240 seconds, begins. The igniter and top-down camera are activated at the beginning of the higher heating ramp as well. The igniter is turned off at the 60 second mark. After the higher heating ramp, the pyrolyzer plate's power is set to 0 and the sample is allowed to cool off for 120 seconds before data collection ends. Figure 1.4 shows the temperature of the pyrolyzer plate during the heating ramps and cooling period for the MFC tests.

3.4.4 MFC Post-Processing

T_{ign} and t_{ign} were determined when the oxygen concentration decreased 0.1 vol% below the mean oxygen concentration of the first 40 seconds of the test. The t_{ign} was compared to visual observations of when the flame was first visible in the experiment. The difference between observed t_{ign} and oxygen concentration decrease time differed by approximately 0.5 seconds across all tests. The observed flame time was used to calculate t_{ext} . Additional information on the operation and data collection of the MFC can be found in De Beer's work [17].

4 Results

4.1 Cone Calorimeter Results

A summary of the Cone Calorimeter results are provided in table 4.1, including t_{ign} , t_{ext} , initial mass, and char yield. For every fabric except the PA Cotton, at least one experiment resulted in a total mass loss greater than the initial mass of the sample. Figure 4.1 shows the samples after each test. For nearly every test, the aluminum foil is damaged, with some tests leaving holes in the aluminum. The masses of the fabric portion of the sample range between 1.73 – 2.89 g, while a 110 x 110 x 0.02 mm sheet of aluminum foil weighs 0.7 – 0.8 g. The loss of aluminum appears to increase the total mass loss of the sample beyond the mass loss of the fabric, a concern discussed in Morgan’s report on the Cone tests [48]. Without a method of accurately separating the fabric char from the damaged aluminum, the actual mass of the fabric char cannot be determined. Therefore, the char yield for samples with total mass loss exceeding 100% are recorded as 0%, even when the samples show char or ash from the fabric.

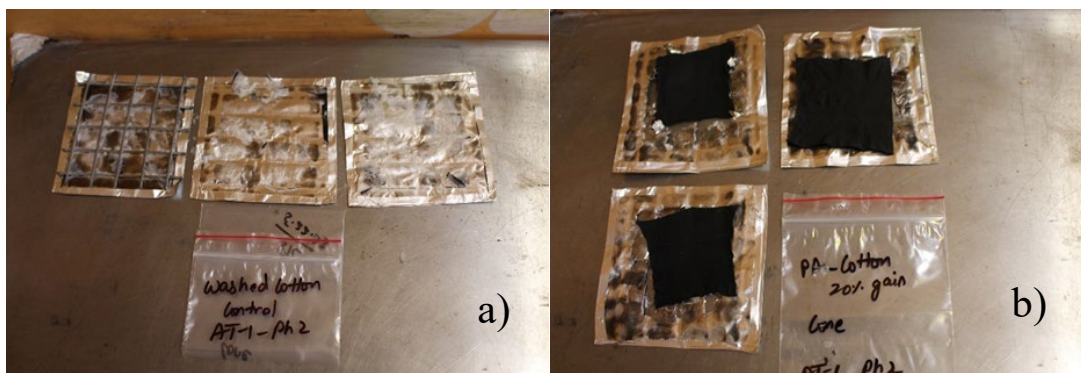




Figure 4.1: Cone Calorimeter Charred Remains for Control Cotton (a), PA Cotton (b), Control Nylon (c), and TA Nylon (d) samples [48]

A 5-point moving average (15 seconds) was used to find the peak HRR and the peak HRR time. The moving average reduces the noise associated with the chaotic nature of solid-mass combustion. The average HRR was integrated between the t_{ign} and t_{ext} for each test, focusing on the flaming portion of the combustion process. There is a delay between the observed extinction of the flame and when the HRR curve returns to the baseline value. It is unclear how much of the post-extinction HRR is caused by the flaming and smoldering combustion processes, so averaging the HRR curve between the ignition and extinction will overpredict the actual average HRR for the flame. However, this averaging technique proved to be the most repeatable way for determining the average HRR across the samples, with the exception of PA Cotton. For PA Cotton, the average was taken for values above 5 kW/m^2 . Figure 4.2 shows the HRR profiles for all three tests conducted for each fabric.

The average and peak HRR for each fabric, normalized by the initial mass and the exposed area (0.0884 m^2), are provided in Table 4.1. The exposed area ignores any fabrics that are hidden by the metal frame in the Cone's sample holder but not the fabric

hidden beneath the metal wire grid. While the samples may shrink and melt so that more or less of the area of the fabric sample is exposed, these interactions are difficult to track during experiments. Using the area of the fabric which is initially exposed for normalization maintains consistent calculations across fabric samples.

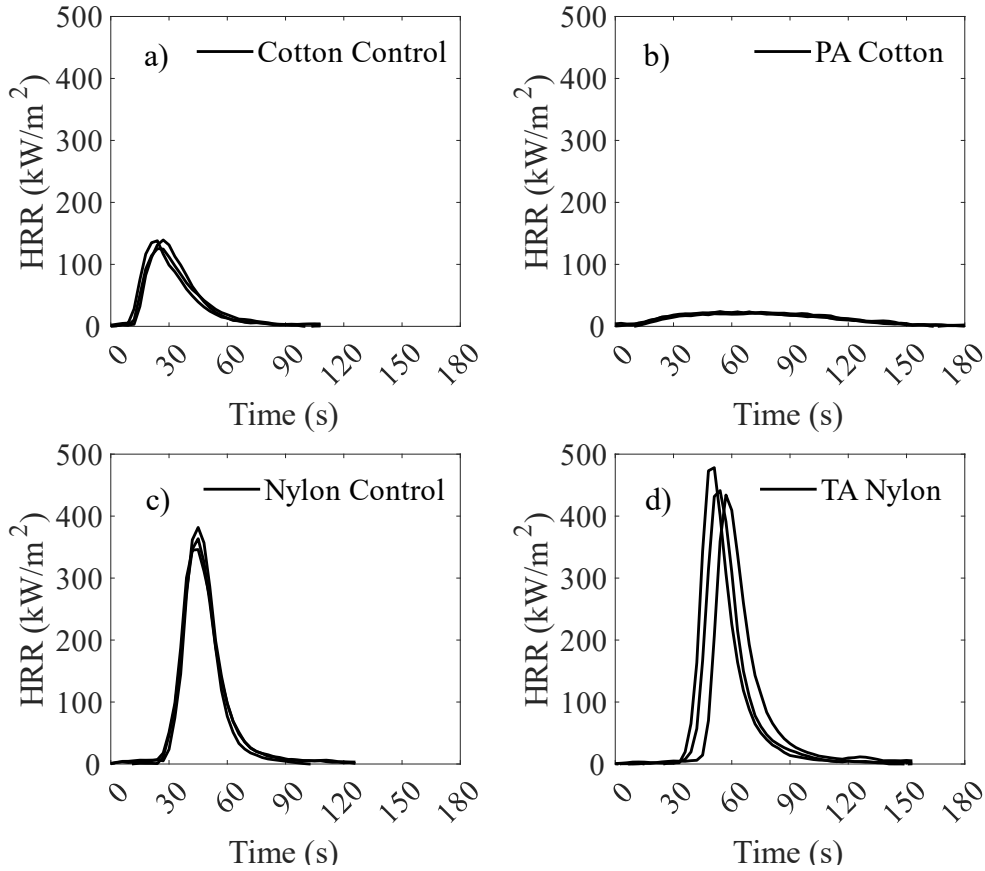


Figure 4.2: Cone Calorimeter HRR curves for Control Cotton (a), PA Cotton (b) Control Nylon (c), and TA Nylon (d) [48]

Figure 4.3 shows the average HRR curves for all four materials in the Cone Calorimeter tests. The precision of the TA Nylon tests is far lower than the other three fabrics, likely due to a high variability in both t_{ign} and pHRR. A delay in ignition time and an increase in pHRR from the Nylon Control sample to the TA Nylon sample is

observed. The shape of the PA Cotton HRR curve is much wider and shorter than the Cotton Control sample, likely indicating that the Cotton PA only underwent a smoldering reaction. The PA Cotton HRR curve appears to rise after the Cotton Control curve, though it's unclear if this is because the PA Cotton's HRR is near the lower detection range of the Cone, because the HRR caused by the PA Cotton's decomposition is smoldering, or because there is a delay in decomposition for the PA Cotton. The Cotton Control sample had an earlier ignition time and lower pHRR than the Nylon Control sample.

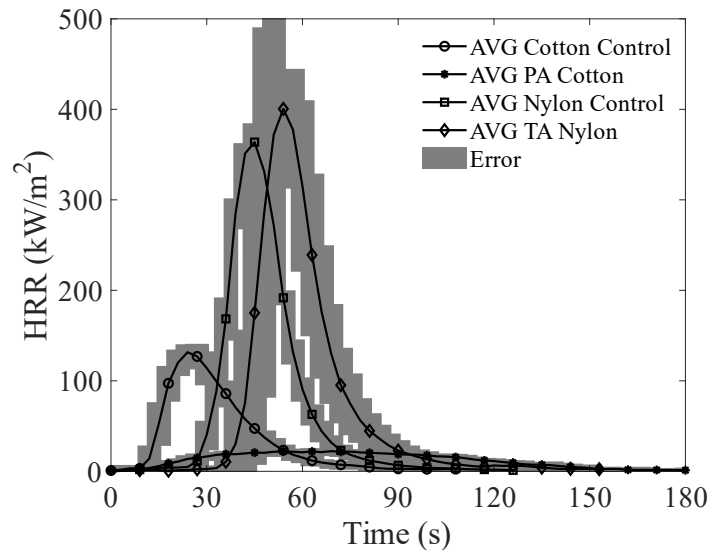


Figure 4.3: Average HRR for all materials in the Cone Calorimeter

The total heat release (THR) was calculated by integrating the HRR curves between the first and last data point where the HRR curve exceeded the baseline value of the graph by two standard deviations. This calculation involves HRR data taken after the extinction time, including both smoldering and flaming combustion oxygen consumption. The total HR was normalized by the initial mass to provide the HOC per initial mass. The HOC per gasified mass was calculated using the following equation,

$$HOC_{gasified} = \frac{HOC_{initial}}{1 - Y_{char}}, \quad (5)$$

Where $HOC_{gasified}$ is the HOC per gasified mass (kW/g), $HOC_{initial}$ is the HOC per initial mass (kW/g), and Y_{char} is the char yield (g/g). The two HOC measurements help differentiate between the HOC for the flaming portion of the fire and the fuel load associated with the total mass of a material. Both HOC's are provided in table 4.1.

Observations on the condensed-phase and gaseous-phase activity of the samples for Cone tests are provided by Alex Morgan. Control Cotton samples began charring and smoking before they ignited and only left ash deposits by the end of the test. Control Nylon samples melted and began to boil before ignition, leaving a black residue on the aluminum foil. PA Cotton samples charred and smoked quickly but did not ignite. The PA Cotton samples shrank down to 2 x 2" flexible squares of carbonized fabric. The TA Nylon samples acted similarly to the Control Nylon samples, with the main notable change being a slight increase in charred remains.

Table 4.1: Summary of Cone Calorimeter Results

	Control Cotton	PA Cotton	Control Nylon	TA Nylon
Initial Weight (g)	1.77 ± 0.04	2.11 ± 0.03	2.16 ± 0.02	2.83 ± 0.05
t_{ign} (s)	9 ± 1	N/A	24 ± 2	36 ± 4
t_{ext} (s)	50 ± 0	N/A	65 ± 1	92 ± 8
pHRR (kW/m^2)	120 ± 5	21.8 ± 1.0	320 ± 9	380 ± 25
pHRR (W/g)	602 ± 23	91.7 ± 5.4	1310 ± 40	1170 ± 50
aHRR (kW/m^2)	72.6 ± 1.4	16.3 ± 0.9	166 ± 9	153 ± 9
aHRR (W/g)	363 ± 6	68.3 ± 4.6	678 ± 32	475 ± 22
Char Yield (%)	0 ± 0	21.4 ± 14.7	1 ± 1	0
HOC Gasified	17.2 ± 0.2	11.3 ± 0.8	31.2 ± 1.6	27.9 ± 0.5
HOC Initial Mass	17.2 ± 0.2	8.91 ± 0.6	30.9 ± 1.5	27.9 ± 0.5

4.2 MCC Results

Figure 4.4 shows the average HRR curves for all four fabrics normalized by the initial mass of the sample. The maximum of a 5-point moving average of the raw HRR data was used to find the peak HRR for each fabric, for similar reasons as the Cone data. The peak HRR for each fabric, normalized by the initial mass and fabric area, are provided in Table 4.2. The area of the fabric samples for the MCC were not measured before testing. To normalize the HRR by area for the tabular results, the HRR was first normalized by the initial mass of the sample and then multiplied by the areal density of the fabric. This normalization technique was used for both pHRR and aHRR. Both

initial mass and Char yield are also provided in table 4.2, calculated using the methods described in section 3.4.2.

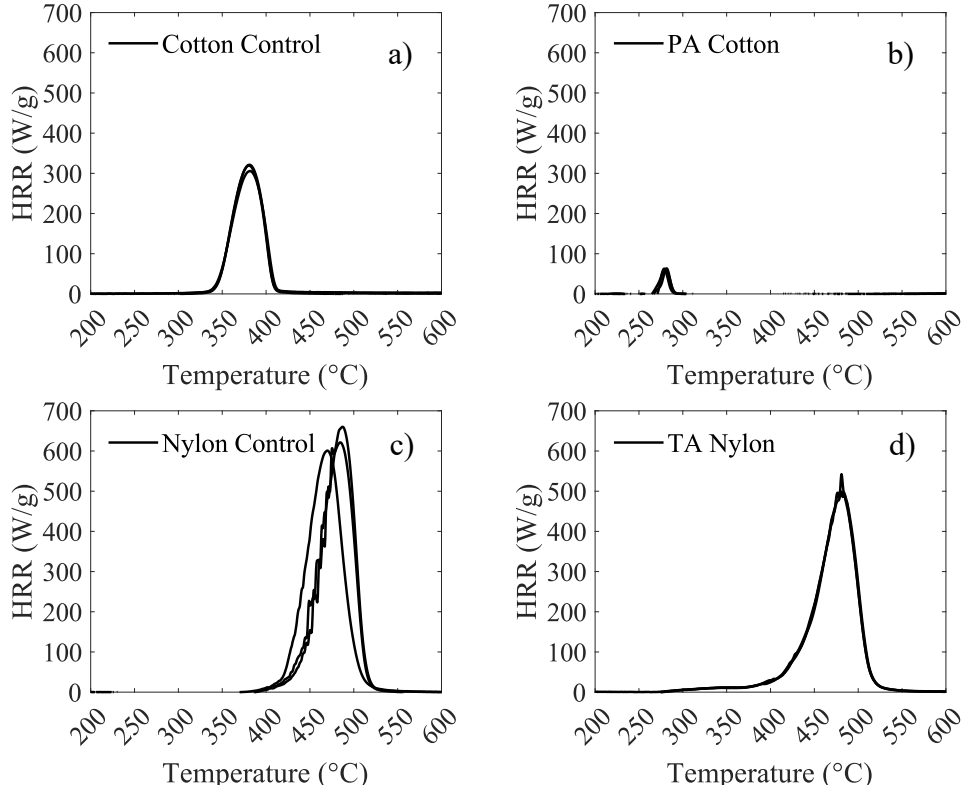


Figure 4.4: MCC HRR Curves for Control Cotton (a), PA Cotton (b), Control Nylon (c), and TA Nylon (d) [49]

The T_{ign} and extinction temperature (T_{ext}) for the MCC were taken when the HRR of the sample exceeded and dropped below 20 W/g. The MCC does not normally provide flame ignition or extinction data, as the combustion chamber doesn't produce a flame. For the Cotton, Nylon, and TA Nylon HRR curves, 20 W/g correlates with a sudden increase in the HRR curves. For PA Cotton, the T_{ign} and T_{ext} were taken at 5 W/g, as the sudden increase in HRR for the PA Cotton sample occurs at this value. The average of the raw HRR data between t_{ign} and t_{ext} was used to calculate the aHRR for

each fabric. T_{ign} , T_{ext} , and aHRR per initial mass are provided in table 4.2 for each fabric.

The THR was calculated by integrating the HRR curves between the first and last point where the HRR curve exceeded the baseline value of the graph by two standard deviations. The baselines for MCC tests were taken from the first 150 data points and the last 150 data points (75 second ranges). The HOC per initial mass was calculated by dividing the THR by the initial mass, while the HOC per gasified mass was calculated using equation (5). Both the HOC per initial mass and gasified mass are provided in table 4.2.

Figure 4.5 shows the average HRR curves for all four materials tested in the MCC. The onset of HRR and pHRR for both fabrics treated with flame retardants is earlier than the control fabrics. The PA Cotton's HRR curve is short in both magnitude and duration, dissimilar to the shape of the PA Cotton curve from figure 4.2. The Nylon Control sample had the least precision amongst the samples. The Cotton Control sample has an earlier onset of combustion and lower pHRR than the Nylon Control sample, as expected.

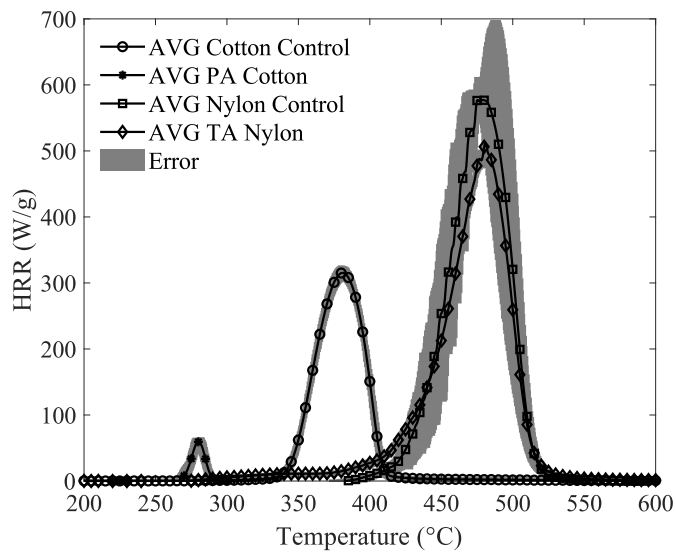


Figure 4.5: Average HRR for all materials in the MCC

While the MCC combustion chamber prevents observation of the condensed-phase activity of the samples, the final charred remains can still provide a some insight into the combustion process. Figure 4.6 shows the fabric samples post-testing. The Control Cotton sample has shrunk and most of the fabric weave features cannot be seen. The PA Cotton sample has decreased its radius less than the Control Cotton and the weave is still visible. Both the Control Nylon and TA Nylon leave behind a think black residue, with the TA Nylon leaving behind a small amount of glassy char near the edges of the crucible.

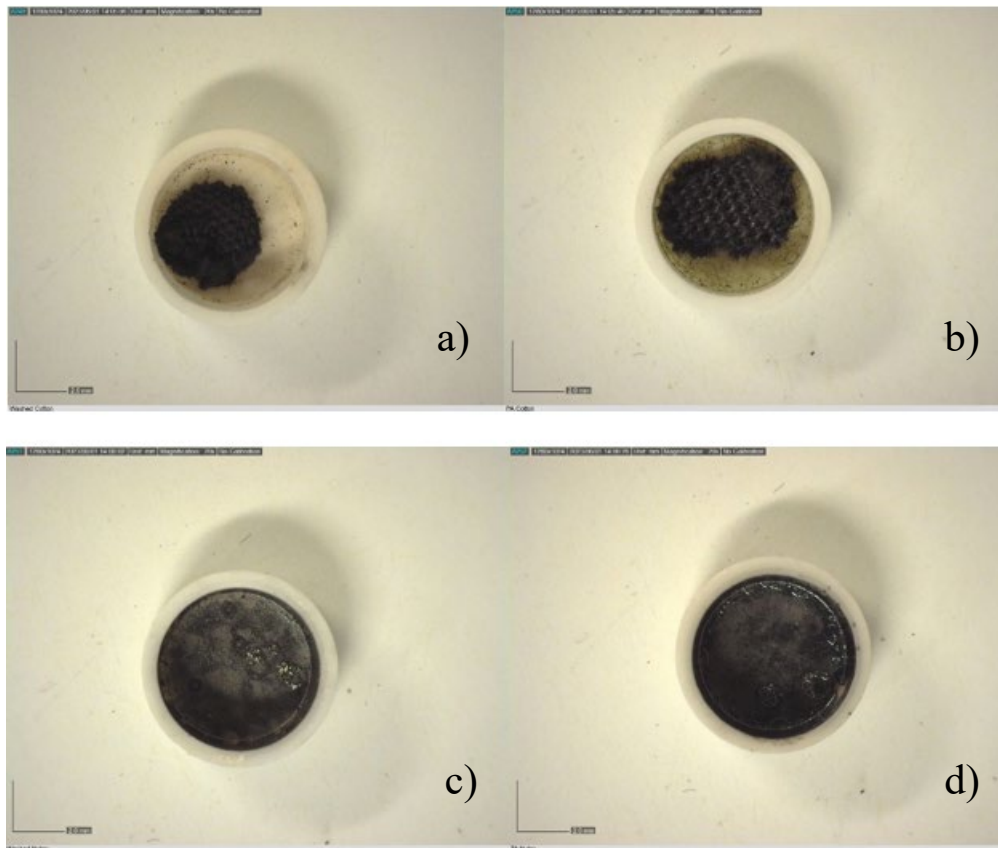


Figure 4.6: MCC Charred remains for Cotton Control (a), PA Cotton (b), Nylon Control (c), and TA Nylon (d) [49]

Table 4.2: Summary of MCC Results

	Cotton Control	PA Cotton	Nylon Control	Nylon TA Nylon
Initial Weight (mg)	5.33 ± 0.27	5.47 ± 0.06	5.5 ± 0.1	5.48 ± 0.12
T _{ign} (°C)	343 ± 21	271 ± 2	422 ± 6	398 ± 2
T _{ext} (°C)	410 ± 3	291 ± 1	516 ± 3	520 ± 1
pHRR (W/g)	315 ± 8	62.3 ± 3	627 ± 30	509 ± 19
pHRR (kW/m ²)	50.4 ± 2	11.7 ± 0.6	132 ± 6	124 ± 3
aHRR (W/g)	203 ± 14	52.2 ± 2.0	317 ± 6	239 ± 2
aHRR (kW/m ²)	32.5 ± 2.0	9.8 ± 0.4	67.2 ± 1.2	58.1 ± 0.5
Char Yield (%)	5.21 ± 0.21	47.7 ± 0.1	1.22 ± 0.07	4.48 ± 0.05
HOC Gassified (kJ/g)	13.0 ± 0.7	0.88 ± 0.11	29.7 ± 0.3	28.8 ± 0.3
HOC Initial Mass (kJ/g)	12.3 ± 0.7	0.46 ± 0.06	29.3 ± 0.2	27.5 ± 0.2

4.3 *MFC Results*

HRR curves were calculated using Method B oxygen consumption calorimetry discussed in section 1.2.4. Figure 4.7 shows the average HRR curves for three tests of each fabric. Method B was used for these calculations to provide HRR curves that don't include significant negative values, as described in De Beer's Thesis [17]. These graphs were normalized by the initial mass of the sample, calculated by subtracting the mass of the fabric and crucible from the mass of the crucible in isolation.

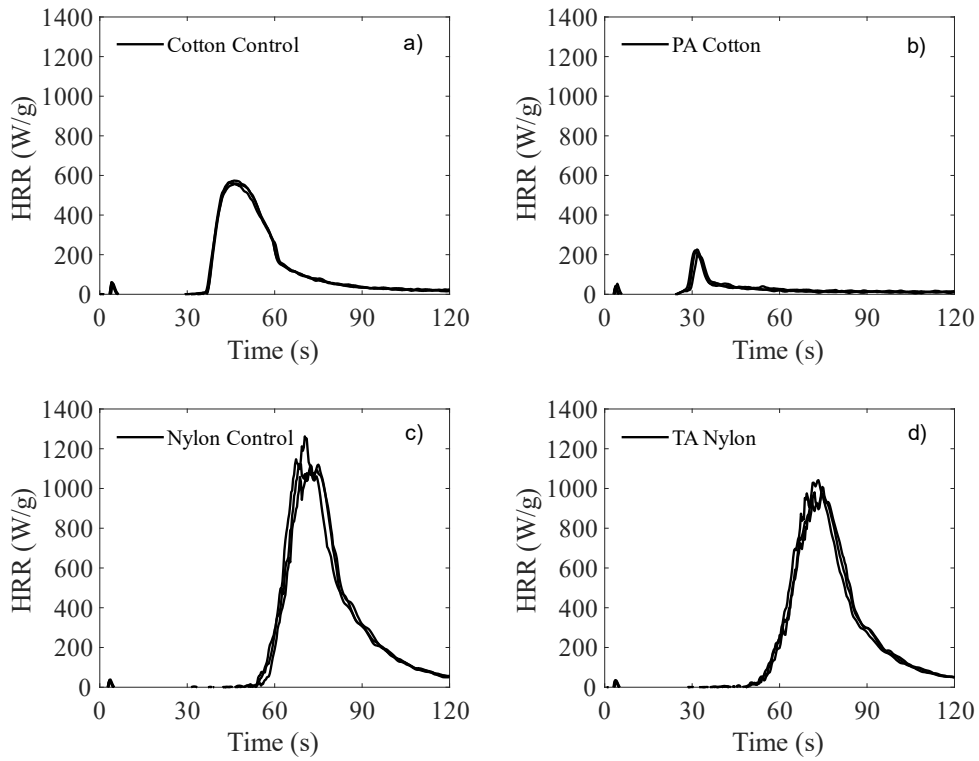


Figure 4.7: MFC HRR Curves for Cotton Control (a), PA Cotton (b), Nylon Control (c), and TA Nylon (d)

The aHRR for each fabric was taken as the average of the HRR curves between t_{ign} and t_{ext} , for similar reasons as the Cone tests. The maximum of a 5-point moving average of the HRR curves was used to find the pHRR for each fabric, for similar reasons as the Cone and MCC. The aHRR and pHRR for each fabric, normalized by initial mass and total fabric area, are provided in table 4.3. The total fabric area for the MFC samples includes the area for all 4 layers combined, 177 mm². The total fabric area was used over the area of the crucible opening as it better correlates with the MCC and Cone HRR values.

The THR was calculated by integrating the HRR curves between the first and last data point where the HRR curve exceeded the baseline value of the graph by two standard deviations. The baseline for the start of each test was the average O₂ concentration for the first 40 seconds, while the baseline for the end of the test was the average oxygen concentration for the last 180 seconds of the test. The THR integration excludes the HRR caused by the igniter turning on. The HOC per initial mass was calculated by dividing the THR by the initial mass, while the HOC per gasified mass was calculated using equation (5). Both the HOC per initial and gasified mass are provided in table 4.3.

Figure 4.8 shows the HRR curves for all four materials. The Cotton Control sample has a shorter ignition time and smaller pHRR than the Nylon Control sample. The introduction of flame retardants to the fabrics leads to decrease in both peak HRR and total curve area for both Cotton and Nylon. The shape of Nylon and TA Nylon HRR curves are similar, while the PA Cotton HRR curve is much steeper than the Control Cotton curve.

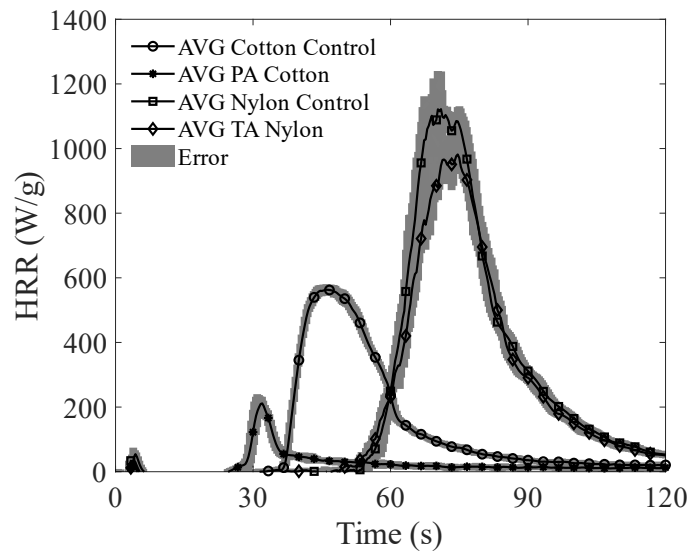


Figure 4.8: Average HRR for all materials in the MFC

Table 4.3: Summary of MFC Results

	Cotton Control	PA Cotton	Nylon Control	TA Nylon
Initial Mass (mg)	28.1 ± 1.2	33.5 ± 0.5	37.7 ± 0.4	42.1 ± 0.4
Char Yield (%)	0	38.2 ± 0.6	0.58 ± 0.816	2.4 ± 0.3
T _{ign} (°C)	381 ± 6	303 ± 4	482 ± 6	481 ± 1
t _{ign} (s)	217 ± 1	209 ± 2	235 ± 1	234 ± 1
pHRR (W/g)	565 ± 7	211 ± 9	1150 ± 70	988 ± 37
pHRR (kW/m ²)	90.2 ± 2.9	40.1 ± 2.2	246 ± 12	236 ± 12
aHRR (W/g)	432 ± 8	166 ± 8	677 ± 57	550 ± 2
aHRR (kW/m ²)	69.2 ± 3.8	31.6 ± 1.9	145 ± 14	131 ± 1
HOC Gasified Mass (kW/g)	14.7 ± 0.3	4.59 ± 0.70	28.2 ± 0.8	26.4 ± 0.2
HOC Initial Mass (kW/g)	14.7 ± 0.3	2.83 ± 0.46	28.0 ± 1.1	25.7 ± 0.1

Each material underwent a unique condensed-phase behavior during the MFC test. The Cotton sample initially darkened into a char before ignition, maintaining its shape and weave. After flame extinction, the char slowly shrunk inwards into a disk of ash with no char remaining. The PA Cotton sample also transformed into char before ignition but did not noticeably decrease in either height or radius. Nylon condensed into a smaller, glassy hemisphere while melting. As the Nylon melted, it began to bubble and eventually boil during the start of ignition. After flame extinction, a thin layer of residue was left on the upper sides of the crucible, which was gone by the end of the experiment. For PA Nylon, while the top half of the sample was still melting, the sample began to expand and produce a black, thick bubble. The bubble continued to balloon out of the inner quartz tube until the side closest to the igniter started to off-gas. Sporadic flaming occurred on the side of the crucible closest to the igniter while the bubble slowly melted back into the crucible. The TA Nylon sample then performed similarly to the Control Nylon sample until leaving a larger charred mass behind.

Each material also underwent unique gas-phase burning behaviors. The Cotton flame began as a small, blue laminar flame, increasing in size to include an orange tip before shrinking back down and extinguishing. The PA Cotton only provided a flash of fire near the igniter for no more than 2 seconds. The Nylon flame began with flashes of light, leading to a small flame that would sporadically jump up in height before returning to the small but consistently growing flame. The sporadic flame height eventually resolved into a axisymmetric laminar flame that decreased in length near extinction. The TA Nylon produced a similar flame pattern to the base Nylon. The charred remains of the tests are provided in Figure 4.9.

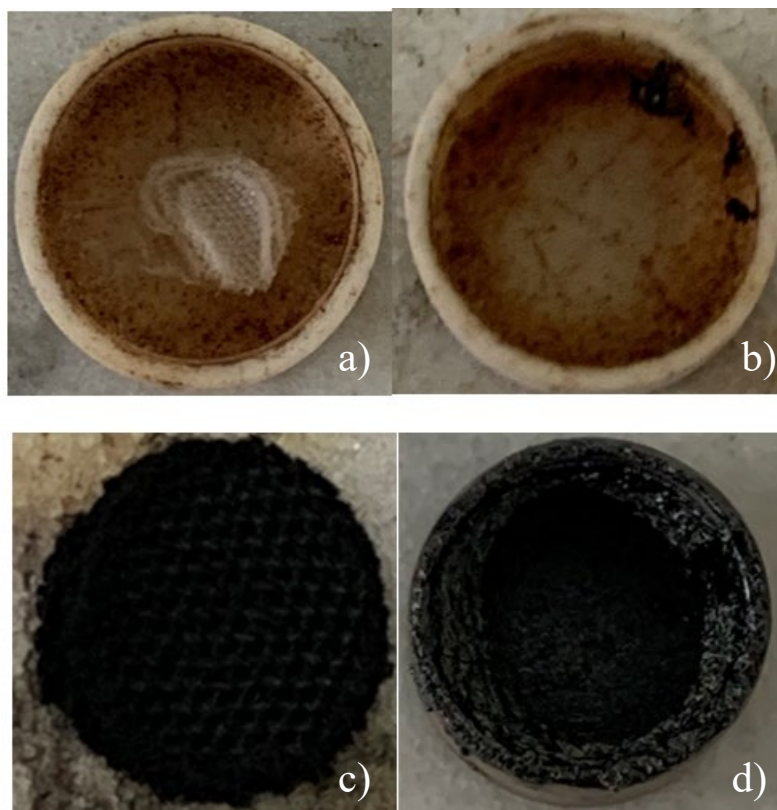


Figure 4.9: MFC Charred remains for Cotton Control (a), Nylon Control (b), PA Cotton (c), and TA Nylon (d)

5 Comparative Analysis and Discussion

This current study aims to investigate the use of the MFC for flammability testing of fabrics by comparing the properties obtained by the MFC with the Cone Calorimeter and MCC. If the MFC produces results that follow similar trends to the Cone Calorimeter and MCC for fabrics with and without flame retardants, then it may be possible to screen future flame-retarded fabrics using the MFC. Comparisons of the onset of ignition, char yield, aHRR, pHRR, and HOC for the three apparatuses are used to investigate our hypothesis.

5.1 *Onset of Ignition*

Ignition temperature is an extensive property of the material that is a function of intensive material properties, the heating rate, the size of the sample, and location of the ignition source. Changes in the heating rate and sample size will impact the distribution of heat within the sample and control the production of volatiles. The time-to-ignition for a sample is even more strongly influenced by heating rate and sample size, as a higher heating rate will decrease the time for a material to reach its ignition temperature.

Correlating the MFC results with the Cone Calorimeter and MCC helps to show if the samples are burning in a similar manner across the three testing apparatuses. A comparison between the time-to-ignition between the three apparatuses is unlikely to provide meaningful data; the heating ramps between the three devices are too dissimilar. However, the time-to-ignition data produced by the Cone Calorimeter can be correlated to the T_{ign} for the MFC and MCC using one-dimensional ignition theory.

For thermally thick solids, the t_{ign} for a polymer can be determined by the following equation,

$$t_{ign} = \frac{(\pi/4)k\rho c(T_{ign}^2 - T_0^2)}{\dot{q}''}, \quad (6)$$

Where \dot{q}'' is the constant heat flux applied to one surface, k is the thermal conductivity, ρ is the density, c is the heat capacity, and T_0 is the ambient temperature. For thermally thin solids, (t_{ign}) is calculated through the following equation,

$$t_{ign} = \frac{\rho c(T_{ign} - T_0)d}{\dot{q}''}, \quad (7)$$

Where d is the depth of the material. While the Cone Calorimeter tests typically assume that the material undergoing pyrolysis is thermally thick, the very thin fabric samples aren't guaranteed to be thermally thick or thermally thin. Without knowing the thermal conductivity of the flame retarded fabrics, we must correlate the t_{ign} of the MFC and MCC to both the t_{ign} and the square root of the t_{ign} of the Cone Calorimeter.

Figure 5.1 shows the average ignition temperature for the MFC and MCC across all fabric tests along with the average ignition time for the Cone Calorimeter across all fabric tests. This figure compares the onset of ignition for all three testing methods under the thermally thin assumption for the Cone Calorimeter. Figure 5.2 shows the same temperature data for the MFC and MCC tests and compares them against the square root of the ignition time for the Cone Calorimeter tests. This figure compares the onset of ignition for all three test methods assuming the thermally thick assumption for the Cone Calorimeter. The ignition temperature for the MFC is consistently higher than the MCC, likely caused by the difference in heating rates and the impact of transportation time. All three testing methods demonstrate an increase in onset of

ignition from the Cotton and Nylon Control samples. Both the MFC and MCC see a decrease in onset of ignition from the Control Cotton samples to the PA Cotton samples. For all three methods, the trends in onset of ignition from the Nylon Control to the TA Nylon samples diverge: the MCC shows a slight decrease in ignition temperature, the MFC shows no significant change in ignition temperature, and Cone Calorimeter shows a large increase in ignition time.

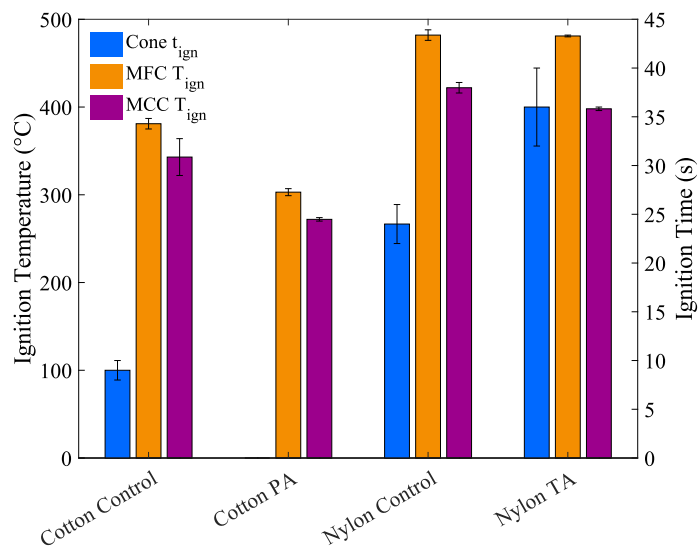


Figure 5.1: Onset of Ignition for Cone (right axis), MFC, and MCC (left axis) Tests across all Fabrics (assuming thermally thin Cone Tests)

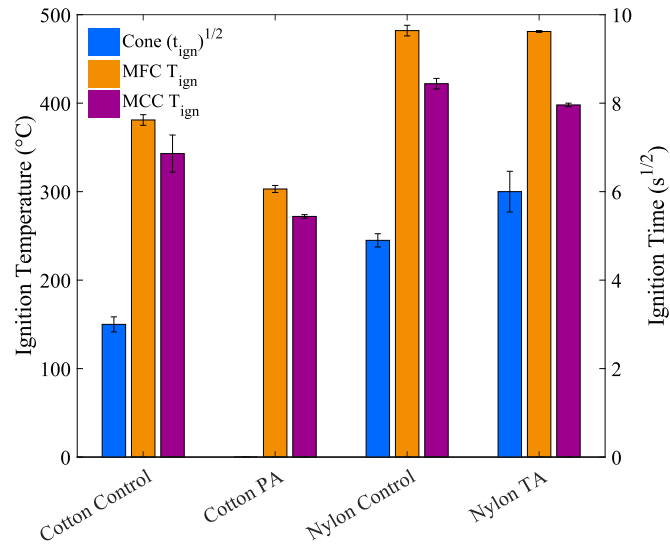


Figure 5.2: Onset of Ignition for Cone (right axis), MFC, and MCC (left axis) Tests across all Fabrics (assuming thermally thick Cone Tests)

To better analyze the differences between the control fabrics and flame-retardant treated fabrics, bar graphs showing the change in the flame parameters from the control fabrics to the treated fabrics are provided. The relative change in flame parameters between the control fabrics to the treated fabrics are calculated using the following equation:

$$Relative\ Change\ (\%) = \frac{A_{FR} - A_{CONTROL}}{A_{CONTROL}}, \quad (8)$$

Where A_{FR} is the average flame parameter for the flame-retardant treated fabric and $A_{CONTROL}$ is the average flame parameter for the control fabric.

Figure 5.3 and Figure 5.4 show the relative change in the Cotton and Nylon onset of ignition with and without flame-retardant treatment using equation (8). Figure 5.3 assumes that the Cone Calorimeter samples are thermally thin, while Figure 5.4 assumes that the Cone Calorimeter samples are thermally thick. The “X” mark over the

Cone Calorimeter bar for the relative Cotton change is meant to clarify that there is no comparison between the Cotton Cone tests.

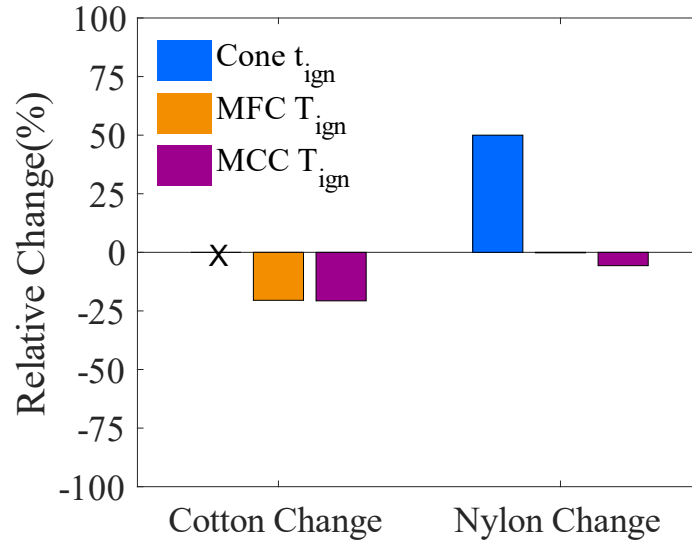


Figure 5.3: Relative Change in Onset of Ignition between the Control to the Flame-Retarded Fabrics, Calculated using Equation (8) (Assuming Thermally Thin Cone Samples)

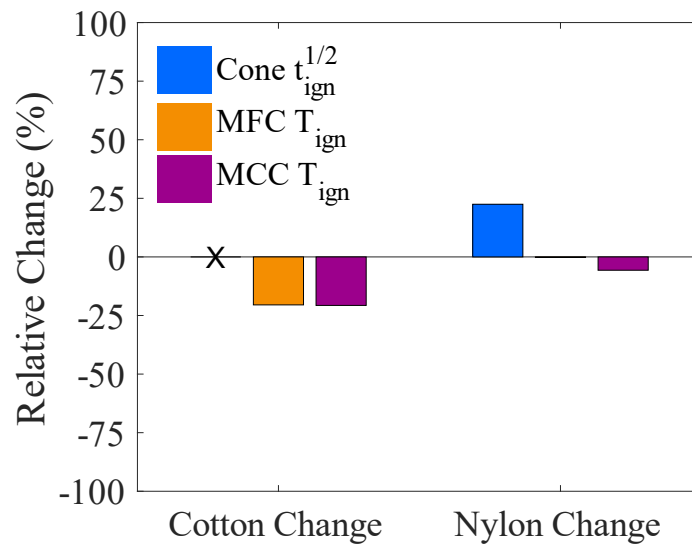


Figure 5.4: Relative Change in Onset of Ignition from the Control to the Flame-Retarded Fabrics, Calculated using Equation (8) (Assuming Thermally Thick Cone Samples)

The difference in the change in onset of ignition caused by the flame-retardant treatments between the three methods is potentially due to differences in how the samples decompose in each test. While the TA Nylon in the MFC causes the formation of a bubble that pops prior to ignition, no bubbles are seen forming in the Cone tests. It's likely that the same viscous carbonaceous layer forms in both tests, and that this layer prevents volatiles from leaving the solid. The reason why the carbonaceous layer in the Cone test doesn't bubble is likely due to differences in how the samples are heated, as the Cone samples are heated through their top surface via thermal radiation and the MFC samples are heated through the bottom via thermal conduction. Visual observations of the carbonaceous layer in the MFC show that it eventually breaks down and either vaporizes or melts back into the nylon liquid pool.

For the MFC tests, because the sample is heated through the bottom layer, the viscous layer near the bottom melts and begins to evaporate before the top of the viscous layer. The production of gases causes the viscous layer to expand upwards, creating a balloon effect. As the viscous layer keeps expanding, it grows thinner and moves closer to the igniter. The additional radiant heat from the igniter causes the portion of the bubble closest to the igniter to weaken enough for volatiles to escape, eventually leading to ignition. For the Cone tests, because the sample is heated through the top layer, the viscous layer insulates the sample beneath it. The viscous layer has to

first break down before a critical mass of volatiles can be produced to begin flaming ignition.

It is also possible that the difference in access to oxygen causes the differences in relative change in onset of ignition between the Nylon and Nylon TA samples for the Cone, MFC and MCC tests. An inert gas flow is used in the MCC to prevent air from reaching the sample. A similar inert gas flow is used in the MFC, although some air entrainment has been identified during this current study. The Cone Calorimeter tests don't include any inert gas to shield the sample, allowing air to flow directly next to the sample. The introduction of oxygen could lead to different chemical activity in the TA Nylon during decomposition, which could in turn change the onset of ignition.

These methods of decomposition are only a hypothesis for now, and it's possible that some other mechanisms are responsible for the difference in ignition time between the MFC and Cone tests for TA Nylon. The viscous layer might have a lower density than solid nylon, which, in the confined space of the crucible, causes the bubble to form instead of gases. Additional tests using apparatus' that focus on material decomposition are required to validate these claims. Furthermore, the lack of visual observation of the condensed-phase activity of samples within the MCC makes it harder to theorize why the TA Nylon samples show a decrease in onset of ignition. However, the visual observations of the condensed-phase activity in the MFC help to diagnose why the trends in onset of ignition are different between the three testing methods. The additional information provided by the MFC helps direct future work for the fabric and flame-retardant fabric treatment flammability research.

5.2 Char Yield

Char yield is an extensive property affected by heating rate, exposure to high temperature, and oxygen concentration. The Cone Calorimeter tests involve an aerobic environment and a high heat flux near the sample. If the test isn't ended immediately after extinction of the flame, the remaining char will continue to smolder. The aluminum foil insulation beneath the Cone Calorimeter sample can also oxidize and char towards the end of the test, artificially reducing the char yield of the sample. While both the MFC and MCC hold their samples in anaerobic environments, the MFC keeps its sample at a higher temperature for a longer period of time than the MCC, and the benchmark tests from section 2.4 indicate that some air is being entrained into the MFC sample.

Figure 5.5 shows the char yield for the Cone, MFC and MCC tests for each fabric. While there does appear to be a decrease in char yield for the Cone tests of Nylon between the control and flame-retardant flame treated fabrics, only one of the three Nylon tests in the Cone showed a mass loss rate less than 100%. The higher char yield for control Nylon over the treated Nylon is likely an instrument error, though this claim should be verified with additional tests. For each fabric, the Cone tests provided the least amount of char yield, followed by the MFC tests and the MCC tests. Cotton PA shows a large increase in char yield over the control cotton, while Nylon TA shows only a small increase in char yield over the control Nylon. These results align with the expectations discussed in the previous paragraph. It should be stated that for De Beer's previous work with the MFC [29], he found similar results in the char yields across most of the polymers tested. Adjustments to the Cone test and MFC tests may produce

similar charring results as the MCC. For this current study, however, it's sufficient to see that the MFC follows the trends in char yield as the Cone and MCC.

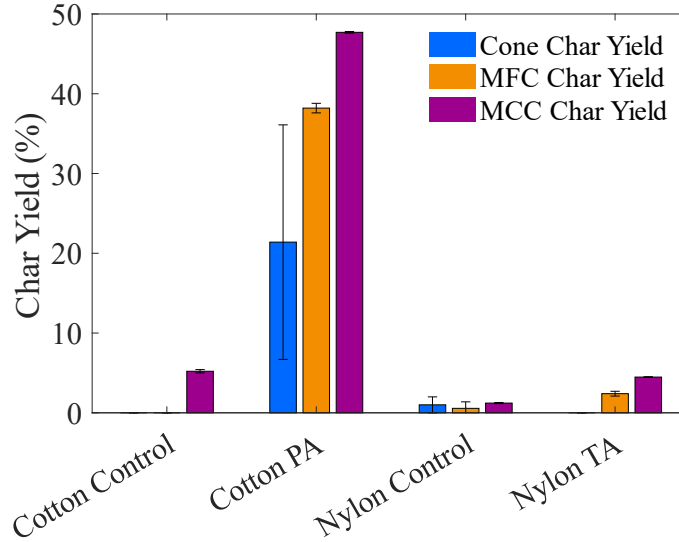


Figure 5.5: Char Yield for Cone, MFC, and MCC Tests across all Fabrics

5.3 Peak and Average HRR

Peak HRR is an important parameter for determining the maximum flame size and heat flux of a fire. Peak HRR helps determine if a fire will grow large enough to ignite flammable materials nearby. Average HRR helps determine the average flow of energy from the fire into the environment and is typically a better method for judging the fire hazard of a material.

For this analysis, the peak and average HRR values normalized by the fabric area rather than initial mass will be used. While both types of normalization of the HRR were presented in section 4 for completeness, the HRR per unit area is more relevant for fabric production and commercialization. The Cone Calorimeter is standardized to use the area normalization for HRR [19], the MFC has used an area normalization before [17], and the MCC typically only uses a normalization by initial mass [31].

While a normalization by area is irregular for the MCC, this method helps to better correlate the HRR results for the three testing devices.

Figure 5.6 shows the peak HRR for Cone, MFC and MCC tests for each fabric normalized by the surface area of the fabric (single face, not both). For the Cotton, Nylon, and Nylon TA samples, the MFC peak HRR lies between the MCC and the Cone values. For the Cotton PA test, the MFC shows the highest peak HRR, likely due to the short but visible ignition observed in the MFC tests. Why the MFC Cotton PA tests show an ignition where the Cone and Nylon tests do not is unclear. It's possible that stacking multiple layers of fabric on top of each other can lead to higher flux of volatiles, especially if the fabric is thermally thin and permeable. It could also be flow turbulence allowing the volatiles to accumulate in the inner quartz tube before reaching a critical concentration for ignition. It has been observed during MFC Cotton tests that a thin, white layer will accumulate in the inner quartz tube before quickly burning out and being replaced by a flame.

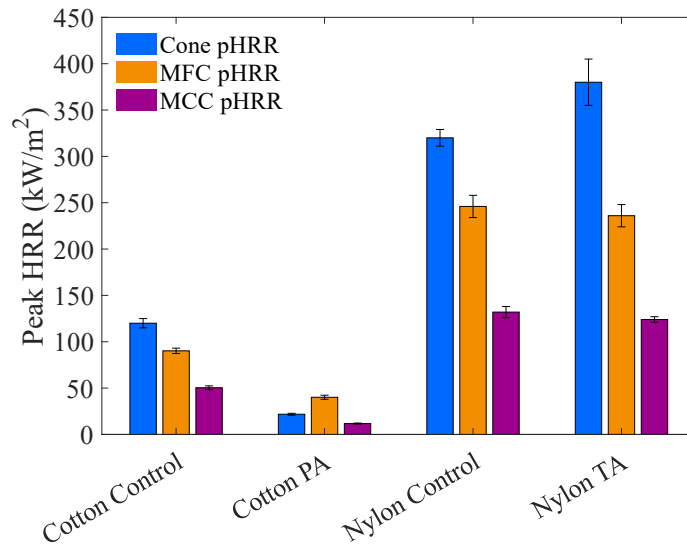


Figure 5.6: Peak HRR for Cone, MFC, and MCC tests for all fabrics normalized by area

It's important to not only analyze the trends across all four fabrics, but also between control fabric and flame retarded fabric. Flame retardants are often judged on their relative change in flame behavior, not the absolute change. Figure 5.7 shows the relative change in pHRR for Cotton and Nylon with and without flame-retardant treatment calculated using equation (8). For Cotton PA, all three devices show the treatment of the fabrics causes a decrease in peak HRR of the same order of magnitude, though the MFC's change is the least drastic. For Nylon, however, the flame-retardant treatment cause the peak HRR for the Cone tests to increases while the MFC and MCC peak HRR's decrease.

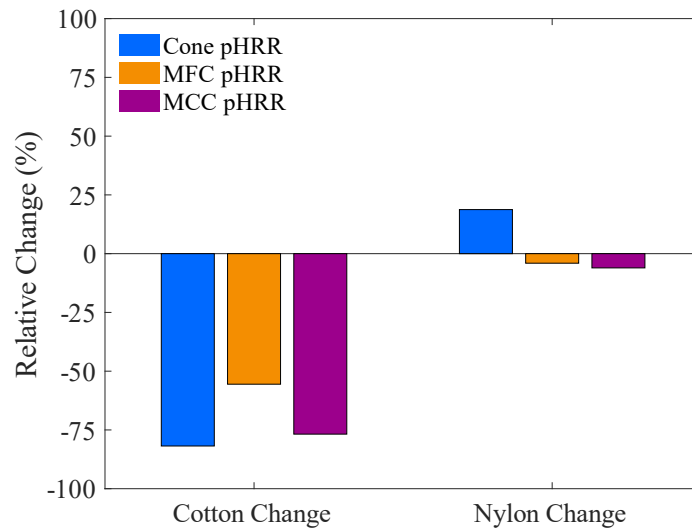


Figure 5.7: Relative Change in pHRR from the Control fabrics to the Flame-Retarded Fabrics, Calculated using Equation (8)

The relative change in Nylon’s pHRR for each testing method follows the same trend as the relative change in onset of ignition for Nylon. It’s likely that both trends are caused by the same phenomenon: the difference in containment and heating rate between the three test methods. During the MFC tests, when the gases begin to escape from the viscous bubble and ignite, the opening is still small and limits the height of the flame. The slow decomposition of the viscous, carbonaceous layer prevents the sharp increase in the release of volatiles seen in the Cone test. For the Cone tests, the viscous layer takes longer to break down, providing more time for the sample to evenly heat. This pre-heated sample releases volatiles faster, leading to a shorter, steeper HRR curve.

The Average HRR profiles help clarify the total size of the fires produced in the fire tests and how the flame retardants change that HRR profile. Figure 5.8 shows the average HRR profiles for Cone, MFC and MCC tests normalized by the fabric area.

The Average HRR graph shows similar trends to the peak HRR graph, with the Cone, MFC, and MCC ranked from highest to lowest HRR for every sample except Cotton PA where the MFC shows the highest HRR. The explanation for these trends are the same as the peak HRR comparison.

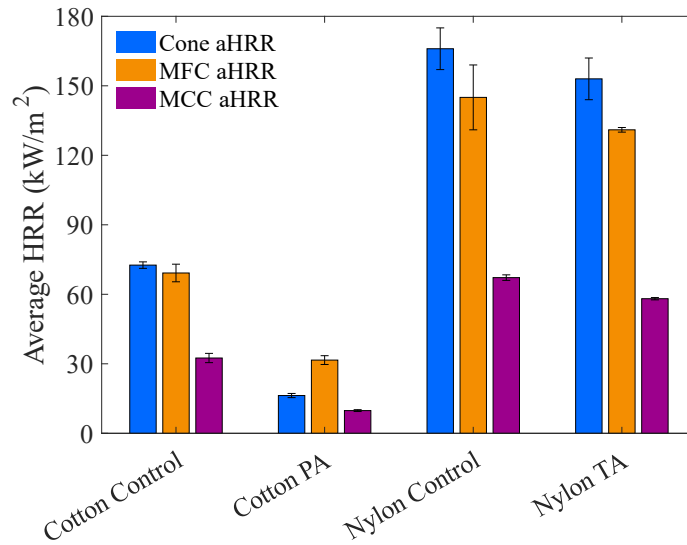


Figure 5.8: Average HRR for Cone, MFC, and MCC tests for all fabrics normalized by area

The trends between the average HRR of the control and flame retarded fabrics, however, show a key difference to the peak HRR story. Figure 5.9 shows the average HRR for the flame retarded fabrics normalized by the average HRR of their respective control fabric calculated using equation (8). The most notable difference between the average and peak HRR trends is the decrease in HRR for the Cone Nylon TA tests compared to the control Nylon. The shorter flame duration for the Cone Nylon TA test ultimately led to a net decrease in the average HRR. All of the fire testing methods show a decrease in average HRR from control fabric to flame retarded fabric.

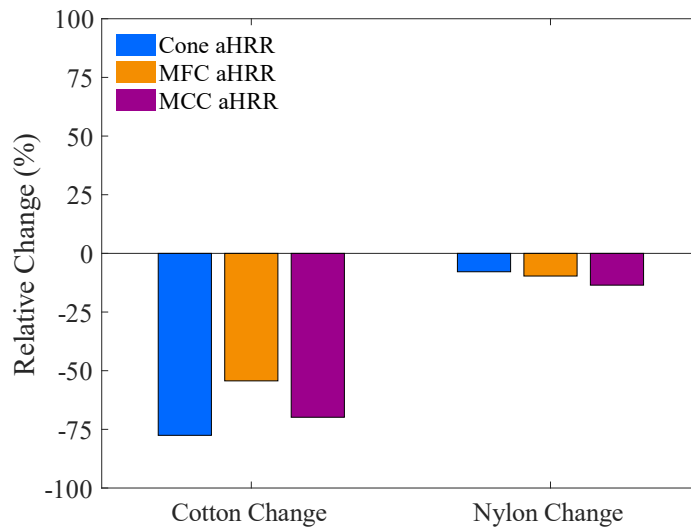


Figure 5.9: Relative Change in aHRR from the Control fabrics to the Flame-Retarded Fabrics, Calculated using Equation (8)

5.4 Heat of Combustion

HOC is an intensive property of a material that helps establish the combustion efficiency and total fuel load of a polymer. HOC is primarily used for determining the fire hazard of a room or container when the geometry and ignitions point are unknown. This makes HOC very useful for determining transportation and storage fire scenarios. When used in conjunction with aHRR, HOC can help determine the burning duration.

Figure 5.10 shows the HOC per gram of the initial sample mass for Cone, MFC, and MCC tests for all fabrics, while Figure 5.11 shows the HOC per gram of gasified mass for the same tests. The HOC normalized by initial mass is more logistically useful for calculating the fire hazard of the polymers in commercial use, while the HOC normalized by gasified mass accounts for differences in char yield between samples. The Cone, MFC and MCC all show similar increases in HOC between the Cotton and Nylon samples. For all fabrics, the Cone tests show the highest HOC per initial mass,

followed by either the MCC or MFC tests. Even when using the HOC per gasified mass, only the TA Nylon samples have the MCC at the highest HOC across all test methods. The Cotton PA tests show a drastic difference in HOC between the tests, with the MCC HOC being less than a tenth of the Cone HOC.

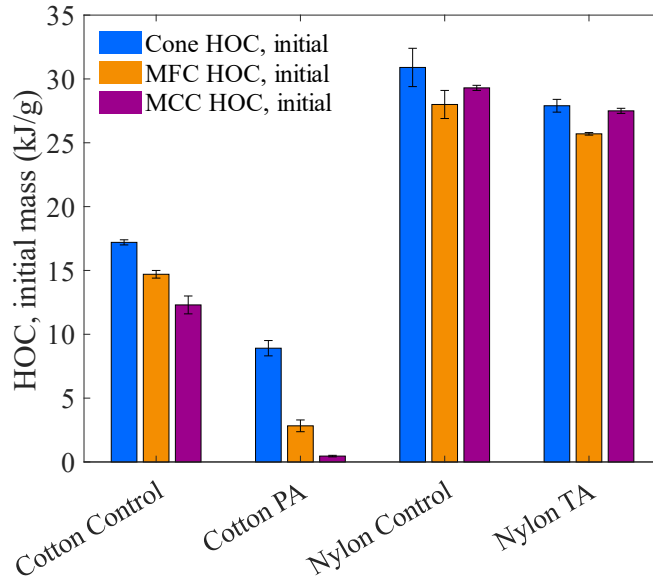


Figure 5.10: HOC per initial mass for Cone, MFC, and MCC tests for all fabrics

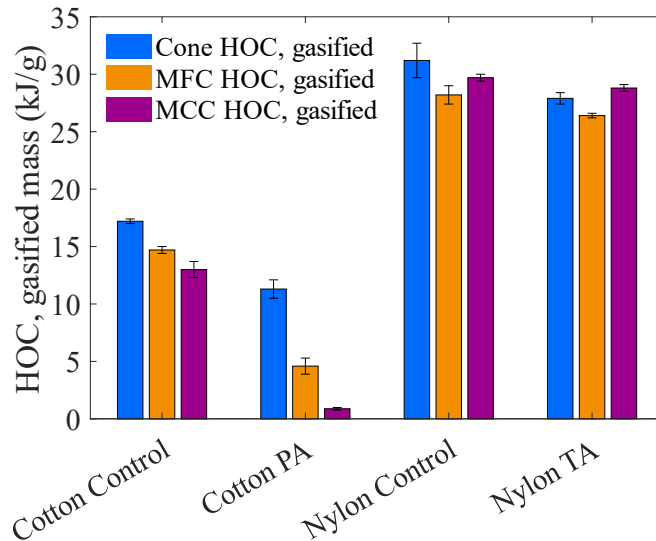


Figure 5.11: HOC per gasified mass for Cone, MFC, and MCC tests for all fabrics

The MCC is typically considered the upper limit for HOC measurements, as the volatiles produced by pyrolysis undergo complete combustion, which has a higher heat release than incomplete combustion. The MCC does have the highest char yield across all fabrics, which does decrease the HOC of the material. For the Nylon samples, the HOC per gasified mass brings the MCC values within the error range of the Cone, while the MFC provides a lower HOC than the other two methods. The discrepancies with the Nylon samples can be assumed to be due to differences in how HOC is calculated for each test.

For the Cotton PA samples, the significant differences between the Cone HOC and the MFC/MCC HOC are difficult to reconcile. The two hypotheses for this odd behavior are that the oxygen consumption of PA Cotton is at the limit for the Cone and MCC devices, or that the different heating rates impact the types of gases produced by PA Cotton. Tests that run near the limit of their devices tend to produce higher error rates, and while the precision Cone and MCC tests aren't low, the error could impact the accuracy of the results. Alternatively, it's possible that the lower heating rate in the MCC favored chemical reactions that produced non-volatile gases compared to the high heating rate for the Cone. Char yield for Cotton is a function of the heating rate [50], so it's possible that composition of the char is also dependent on the heating rate. Future work will investigate both of these hypotheses by increasing the layer depth for the Cone and MCC tests to overcome the low oxygen concentration concern, along with analysis of the char composition for the MCC and Cone to see what percentage of carbon and hydrogen is still present.

Figure 5.12 show the relative change in HOC per initial mass between the control and flame-retardant treated fabrics. Figure 5.13 shows the relative change in HOC per gasified mass between the control and flame-retardant treated fabrics. The Cone, MFC and MCC all show small decreases in HOC for the introduction of Tannic Acid in Nylon. It should be noted that the Nylon TA is a 9% mass increase over the control Nylon, meaning that the small decrease in HOC in each apparatus is likely only due to dilution of the flammable portion of the sample.

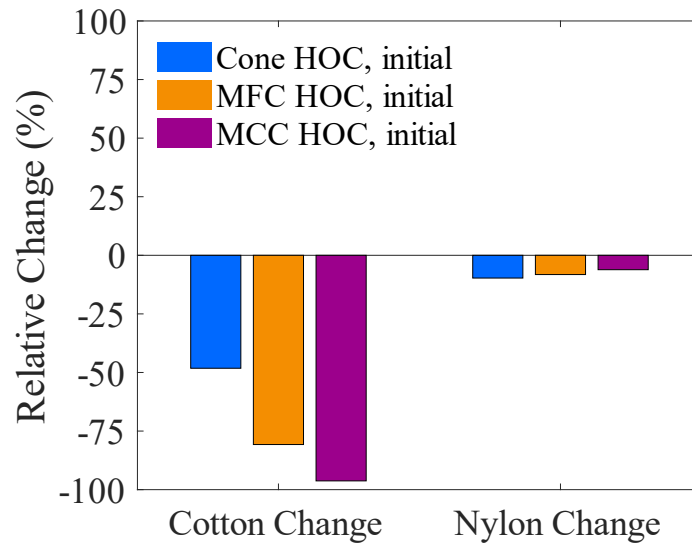


Figure 5.12: Relative Change in HOC per initial mass from the Control fabrics to the Flame-Retarded Fabrics, Calculated using Equation (8)

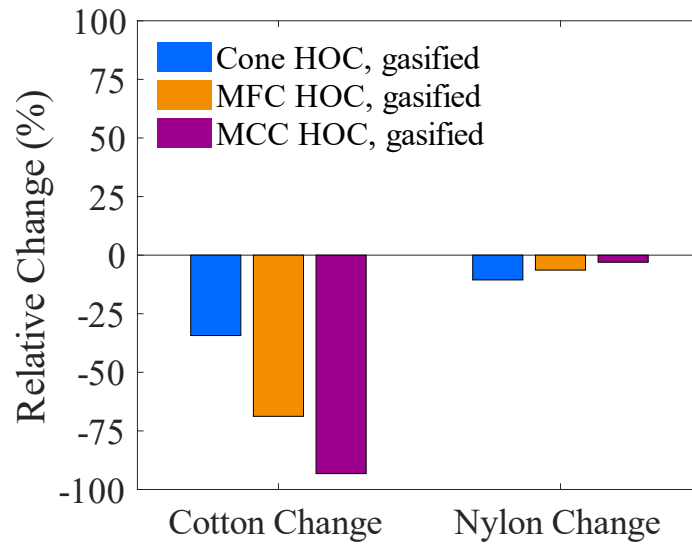


Figure 5.13: Relative Change in HOC per gasified mass from the Control fabrics to the Flame-Retarded Fabrics, Calculated using Equation (8)

6 Conclusion and Future Work

6.1 *Conclusion*

This study examined the use of the MFC for testing fabrics for flame properties to expand the use case of the apparatus. Tests were conducted on Cotton, Nylon, Cotton with 20% Phosphoric Acid gain, and Nylon with 9% Tannic Acid gain. Updates and a status check for the design of the MFC were discussed, including changes to the igniter system, updating the seal between the combustion chamber and the downstream flow to the gas cards, checking the repeatability of the pyrolyzer system, and checking the repeatability of the MFC against its previous iteration. While there were some concerns regarding the repeatability of the MFC across different pyrolyzers, the consistency of a single pyrolyzer was verified. The optimal method for burning fabrics in the MFC was investigated. Using four layers of fabric per sample and tamping the fabrics together provides consistent results across each fabric tested.

The results of the MFC's fabric tests were compared with the tests of the same fabrics using the Cone Calorimeter and the MCC to see if the MFC shows similar trends in flammability parameters for untreated and treated fabrics. For the untreated fabrics, the MFC shows similar results and trends in the onset of ignition, char yield, peak HRR, average HRR, and heat of combustion as both the Cone Calorimeter and the MCC, with the MFC values almost always lying between the Cone and MCC values. For the flame-retardant treated fabrics and the relative change in flammability parameters between the control fabrics and the treated fabrics, the trends in flammability parameters aren't always the same across all three methods. The Cone Calorimeter TA Nylon samples show an increase in both onset of ignition and peak HRR over the control Nylon, while

the MFC and MCC Nylon samples show decreases in both parameters. The average and peak HRR for PA Cotton in the MFC is much higher than the Cone Calorimeter or MCC tests. The HOC for PA Cotton differs by an order of magnitude across the three testing methods. These significant discrepancies in values highlight the difficulties in accurately characterizing the flammability parameters for flame-retardant treated fabrics. The visual observations of the MFC's condensed- and gas-phase activity help inform why the three testing methods may show different trends in their flammability parameters. Those observations help the researchers understand the how the flame retardants reduce the flammability of the fabrics and may help researchers predict the burning behavior of samples in situations outside of the three bench scale tests. Ultimately the MFC provides quantitative flammability data on fabrics as reliable as either the Cone Calorimeter or MCC while providing additional qualitative data on how the samples burn.

6.2 *Future Work*

Additional updates to the design of the MFC are critical to future use of the apparatus. The current pyrolyzer system needs to be adjusted to reduce the production time of new pyrolyzers and increase repeatability of the heating ramp. The oxidation of char in the crucible needs to be reduced, either by reducing the entrainment of air into the inner quartz tube or limiting the amount of time the pyrolyzer stays at high temperatures. A larger connection piece between the combustion chamber and the downstream flow line needs to be constructed to house a larger inflatable seal. A device for identifying the thermal conductivity of samples in a modified MFC test would help

expand the MFC from comparisons with other devices to providing a fire growth model on its own.

For future fabric testing, additional tests on fabrics used in this study will be done with modified methods for the Cone, MCC and MFC to better understand these preliminary results. When the separated Cotton and Nylon samples are better understood, the next step will be to test a 50% blend of Nylon and Cotton, “Nyco”, with Phosphoric Acid and Tannic Acid applications. Comparisons between the MFC results with standard aimed at ranking polymer flammability, such as the Vertical Flame Test [6] and the Mannequin Flame Test [7]. The long-term goal of this research is to provide a link between MFC tests and real fire incidents and hazards.

7 Bibliography

- [1] Lazar, S.T., Kolibaba, T.J. & Grunlan, J.C. Flame-retardant surface treatments. *Nat Rev Mater* 5, 259–275 (2020). <https://doi.org/10.1038/s41578-019-0164-6>.
- [2] J. Egan, S. Salmon, Strategies and progress in synthetic textile fiber biodegradability. *SN Appl. Sci.* 4, 22 (2022). <https://doi.org/10.1007/s42452-021-04851-7>.
- [3] C.D. Papaspyrides, P.T.A.-T.T.- Kiliaris, Polymer green flame retardants, (2014). <http://public.ebib.com/choice/publicfullrecord.aspx?p=1770235>.
- [4] J. Alongi, F. Carosio, G. Malucelli, Current emerging techniques to impart flame retardancy to fabrics: An overview, *Polymer Degradation and Stability*, Volume 106, (2014), 138-149, ISSN 0141-3910, <https://doi.org/10.1016/j.polymdegradstab.2013.07.012>.
- [5] R. Horrocks, Flame retardant challenges for textiles and fibres: New chemistry versus innovatory solutions, *Polymer Degradation and Stability*, Volume 96, Issue 3, (2011), 377-392, ISSN 0141-3910, <https://doi.org/10.1016/j.polymdegradstab.2010.03.036>.
- [6] ASTM D6413, Standard Test Method for Flame Resistance of Textiles (Vertical Test), 2022
- [7] ASTM F1930, Standard Test Method for Evaluation of Flame-Resistant Clothing for Protection Against Fire Simulations Using an Instrumented Manikin, 2023
- [8] A.R. Horrocks, The Potential for Bio-Sustainable Organobromine-Containing Flame Retardant Formulations for Textile Applications-A Review, *Polymers*, (2020), 12, 10.3390/polym12092160.
- [9] A.B. Morgan, M.L. Galaska, Flammability testing of wool/cellulosic and wool/synthetic fiber blends: Vertical flame spread and heat release results, *Journal of Fire Sciences* (2020), 38(6):522-551, doi:10.1177/0734904120954013.
- [10] C. K. Kundu, Z. Li, L. Song, Y. Hu, An overview of fire retardant treatments for synthetic textiles: From traditional approaches to recent applications, *European Polymer Journal*, Volume 137, (2020), 109911, ISSN 0014-3057, <https://doi.org/10.1016/j.eurpolymj.2020.109911>.
- [11] S. Chang, R.P. Slopek, B. Condon, et al., Surface coating for flame-retardant behavior of cotton fabric using a continuous layer-by-layer process, *Ind Eng Chem Res* (2014), 53: 3805–3812.
- [12] M. Leistner, A.A. Abu-Odeh, S.C. Rohmer, et al., Water-based chitosan/melamine polypropylene multilayer nanocoating that extinguishes fire on polyester-cotton fabric, *Carbohydr Polym* (2015), 130: 227–232.
- [13] G. Laufer, C. Kirkland, A.B. Morgan, et al., Intumescent multilayer nanocoating, made with renewable polyelectrolytes, for flame-retardant cotton, *Biomacromolecules* (2012), 13: 2843–2848.
- [14] X. Ding, Design and implementation of the flaming combustion calorimeter, *ProQuest Dissertations & Theses Global*, (2013), (1505378457).

- <https://www.proquest.com/dissertations-theses/design-implementation-flaming-combustion/docview/1505378457/se-2>
- [15] F. Raffan-Montoya, X. Ding, S.I. Stoliarov, R.H. Kraemer, Measurement of heat release in laminar diffusion flames fueled by controlled pyrolysis of milligram- sized solid samples: Impact of bromine- and phosphorus-based flame retardants, (2015) 4660–4670, doi:<https://doi.org/10.1016/j.combustflame.2015.09.031>.
- [16] F. Raffan-Montoya, S.I. Stoliarov, S. Levchik, E. Eden, Screening flame retardants using milligram-scale flame calorimetry, *Polym. Degrad. Stab.* 151 (2018), 12–24. doi:<https://doi.org/10.1016/j.polymdegradstab.2018.02.018>.
- [17] J. A. De Beer, Milligram-scale flame calorimetry: Novel design of a pyrolyzer system used to emulate the burning behavior exhibited by coupon-sized cone calorimetry samples, ProQuest Dissertations & Theses Global, (2020), (2454590140), <https://www.proquest.com/dissertations-theses/milligram-scale-flame-calorimetry-novel-design/docview/2454590140/se-2>
- [18] C. Huggett, Estimation of rate of heat release by means of oxygen consumption measurements, *Fire Mater.* 4 (1980) 61–65. doi:10.1002/fam.810040202.
- [19] ASTM E1354, Standard Test Method for Heat and Visible Smoke Release Rates for Materials and Products Using an Oxygen Consumption Calorimeter, (2019).
- [20] D. F. Swinehart, “The Beer-Lambert Law.” *Journal of Chemical Education* 39 (1962), 333.
- [21] Cone Calorimeter, National Institute of Standards and Technology, December 3, 2021, <https://www.nist.gov/laboratories/tools-instruments/cone-calorimeter>
- [22] R.J. Bray, S. Tretsiakova-McNall, & J. Zhang, The Controlled Atmosphere Cone Calorimeter: A Literature Review, *Fire Technol*, (2023), <https://doi.org/10.1007/s10694-023-01423-6>
- [23] Barbrauskas, The Rational Development of Bench-Scale Fire Tests for Full-Scale Fire Protection, *Fire Safety Science – Proceedings of the Second International Symposium*, International Association for Fire Safety Science, 1989.
- [24] R. Lyon, R. Walters, A Microscale Combustion Calorimeter, Federal Aviation Administration, February 2002.
- [25] R.E. Lyon, R.N. Walters, and S.I. Stoliarov, Screening flame retardants for plastics using microscale combustion calorimetry, *Polym Eng Sci*, (2007), 47: 1501-1510, <https://doi.org/10.1002/pen.20871>
- [26] J. H. Cho, V. Vasagar, K. Shanmuganathan, A. R. Jones, S. Nazarenko, and C. J. Ellison, *Chemistry of Materials*, (2015), 27 (19), 6784-6790, DOI: 10.1021/acs.chemmater.5b03013
- [27] C. Q. Yang, Q. He, Applications of micro-scale combustion calorimetry to the studies of cotton and nylon fabrics treated with organophosphorus flame retardants, *Journal of Analytical and Applied Pyrolysis*, Volume 91, Issue 1, (2011), Pages 125-133, ISSN 0165-2370, <https://doi.org/10.1016/j.jaap.2011.01.012>.

- [28] H. Lu and C.A. Wilkie, Fire performance of flame retardant polypropylene and polystyrene composites screened with microscale combustion calorimetry. *Polym. Adv. Technol.*, (2011), 22: 14-21. <https://doi.org/10.1002/pat.1697>
- [29] H. Lu, C. A. Wilkie, Study on intumescent flame retarded polystyrene composites with improved flame retardancy, *Polymer Degradation and Stability*, Volume 95, Issue 12, (2010), Pages 2388-2395, ISSN 0141-3910, <https://doi.org/10.1016/j.polymdegradstab.2010.08.022>.
- [30] R. A. Mensah, V. Shanmugam, S. Narayanan, J. S. Renner, K. Babu, R. E. Neisiany, M. Försth, G. Sas, O. Das, A review of sustainable and environment-friendly flame retardants used in plastics, *Polymer Testing*, Volume 108, (2022), 107511, ISSN 0142-9418, <https://doi.org/10.1016/j.polymertesting.2022.107511>.
- [31] ASTM D7309, Standard Test Method for Determining Flammability Characteristics of Plastics and Other Solid Materials Using Microscale Combustion Calorimetry, (2019).
- [32] P Singh, Science of Fire Tetrahedron & Chain Reaction of Fire Mechanism, *Fire Engineer*, Volume 39, Issue 2, 7-9, ISSN 0970-3969.
- [33] S.R. Turns, *An introduction to combustion: Concepts and applications* (2nd ed.), (2000), McGraw-Hill.
- [34] D. Price, G. Anthony, P. Carty, *Introduction: polymer combustion, condensed phase pyrolysis and smoke formation, Fire retardant materials*, Boca Raton FL: CRC Press LLC, (2001), P 1---30.
- [35] S. Bourbigot, S. Duquesne, Fire retardant polymers: recent developments and opportunities. *J Mater Chem* (2007); 17: 2283---300.
- [36] R. Sonnier, B. Otazaghine, L. Ferry, Study of the combustion efficiency of polymers using a pyrolysis--- combustion flow calorimeter.
- [37] Gunnar Heskestad, Engineering relations for fire plumes, *Fire Safety Journal*, Volume 7, Issue 1, (1984), Pages 25-32, ISSN 0379-7112, [https://doi.org/10.1016/0379-7112\(84\)90005-5](https://doi.org/10.1016/0379-7112(84)90005-5).
- [38] Jan L. Lyche, Carola Rosseland, Gunnar Berge, Anuschka Polder, Human health risk associated with brominated flame-retardants (BFRs), *Environment International*, Volume 74, (2015), Pages 170-180, ISSN 0160-4120, <https://doi.org/10.1016/j.envint.2014.09.006>.
- [39] Zhen Xiu Zhang, Jin Zhang, Bing-Xue Lu, Zhen Xiang Xin, Chang Ki Kang, Jin Kuk Kim, Effect of flame retardants on mechanical properties, flammability and foamability of PP/wood-fiber composites, *Composites Part B: Engineering*, Volume 43, Issue 2, (2012), Pages 150-158, ISSN 1359-8368, <https://doi.org/10.1016/j.compositesb.2011.06.020>.
- [40] I.M. Salin and J.C. Seferis, Kinetic analysis of high-resolution TGA variable heating rate data. *J. Appl. Polym. Sci.*, (1993), 47: 847-856. <https://doi.org/10.1002/app.1993.070470512>
- [41] V. Seebauer, J. Petek, G. Staudinger, Effects of particle size, heating rate and pressure on measurement of pyrolysis kinetics by thermogravimetric analysis, *Fuel*, Volume 76, Issue 13, (1997), Pages 1277-1282, ISSN 0016-2361, [https://doi.org/10.1016/S0016-2361\(97\)00106-3](https://doi.org/10.1016/S0016-2361(97)00106-3).

- [42] R. Mehrabian, Robert Scharler, Ingwald Obernberger, Effects of pyrolysis conditions on the heating rate in biomass particles and applicability of TGA kinetic parameters in particle thermal conversion modelling, *Fuel*, Volume 93, (2012), Pages 567-575, ISSN 0016-2361, <https://doi.org/10.1016/j.fuel.2011.09.054>.
- [43] Y. Zhang, Y.C. Wang, C.G. Bailey, A.P. Taylor, Global modelling of fire protection performance of intumescent coating under different cone calorimeter heating conditions, *Fire Safety Journal*, Volume 50, (2012), Pages 51-62, ISSN 0379-7112, <https://doi.org/10.1016/j.firesaf.2012.02.004>.
- [44] P. Patel, T.R. Hull, A.A. Stec, and R.E. Lyon, Influence of physical properties on polymer flammability in the cone calorimeter, *Polym. Adv. Technol.*, (2011), 22: 1100-1107, <https://doi.org/10.1002/pat.1943>
- [45] O.P. Korobeinichev, A.A. Paletsky, M.B. Gonchikzhapov, R.K. Glaznev, I.E. Gerasimov, Y.K. Naganovsky, I.K. Shundrina, A.Yu. Snegirev, R. Vinu, Kinetics of thermal decomposition of PMMA at different heating rates and in a wide temperature range, *Thermochimica Acta*, Volume 671, (2019), Pages 17-25, ISSN 0040-6031, <https://doi.org/10.1016/j.tca.2018.10.019>.
- [46] R.A. Mensah, Q. Xu, S. Asante-Okyere, et al, Correlation analysis of cone calorimetry and microscale combustion calorimetry experiments, *J Therm Anal Calorim*, 136, 589–599, (2019), <https://doi.org/10.1007/s10973-018-7661-5>
- [47] Sourabh Kulkarni, Zhiyu Xia, Shiran Yu, Weeradech Kiratitanavit, Alexander B. Morgan, Jayant Kumar, Ravi Mosurkal, and Ramaswamy Nagarajan, *ACS Applied Materials & Interfaces*, (2021), 13 (51), 61620-61628 DOI: 10.1021/acsami.1c16474
- [48] A.B. Morgan, Cone Calorimeter Testing of UML-Army Fabric Samples, University of Dayton Research Institute, (2023), 9001:2015.
- [49] A.B. Morgan, MCC Testing of UML Army Fabrics, University of Dayton Research Institute, (2023), 9001:2015.
- [50] Jenny Alongi and Giulio Malucelli, Cotton Flame Retardancy: State of the Art and Future Perspectives, *RSC Advances*, (2015), Pages 24239-24263, <https://doi-org.proxy-um.researchport.umd.edu/10.1039/C5RA01176K>